Science and Technology for Energy Transition **78**, 5 (2023)

https://doi.org/10.2516/stet/2023003

Available online at:
stet-review.org

REGULAR ARTICLE OPEN ACCESS

Understanding the performance, emissions, and combustion behaviors of a DI diesel engine using alcohol/hemp seed oil biodiesel/diesel fuel ternary blends: Influence of long-chain alcohol type and concentration

Zeki Yilbaşi[1,*], Murat Kadir Yeşilyurt[2,*], Mevlüt Arslan[2], and Hayri Yaman[3]

[1] Department of Automotive Technology, Yozgat Bozok University, Yozgat 66200, Turkey
[2] Department of Mechanical Engineering, Yozgat Bozok University, Yozgat 66200, Turkey
[3] Department of Automotive Technology, Kırıkkale University, Kırıkkale 71450, Turkey

Received: 27 November 2022 / Accepted: 30 January 2023

Abstract. In this study, it was aimed to examine the influences of biodiesel–diesel-higher alcohol (1-pentanol, 1-hexanol, and 1-heptanol) blends on the performance, emission and combustion behaviors of a single-cylinder diesel engine. The tests were performed at a fixed speed of 1500 rpm and variable loads (25%, 50%, 75%, and 100%). For the tests, 80% diesel and 20% hemp seed oil biodiesel were blended and called as B20. Biodiesel fuel was produced by transesterification from hemp seed oil in the presence of methanol and potassium hydroxide for the preparation of B20 binary test fuel and other ternary fuels. Furthermore, nine ternary blend fuels [20% HSOB + 70%, 60% and 50% diesel, respectively + 10%, 20% and 30% higher alcohol (pentanol, hexanol and heptanol) respectively] were prepared. The calculations made with the experimental data revealed that the minimum brake specific energy consumption values were 12,48 MJ/kW h, 13,06 MJ/kW h, 13,27 MJ/kW h, 13,35 MJ/kW h, 13,47 MJ/kW h, and 13,59 MJ/kW h, respectively, for diesel fuel at full load, for fuels B20, B20Hx10, B20Hp10, B20Hx20 and B20Pe10, the maximum brake thermal efficiency values were obtained as 28.85%, 27.56%, 27.14%, 26.97%, 26.73% and 26.49%, respectively, for the same fuels at the same load. The increment in higher alcohol concentration in the blend delayed start of combustion and therefore the ignition delay period was prolonged. In the fuel line pressure data, changes were observed depending on the amount, viscosity and density of the fuel. Furthermore, B20Hx10 and B20Hp10 fuels gave the maximum in-cylinder pressure, heat release rate, average gas temperature and pressure rise rate values after diesel and biodiesel. The addition of biodiesel and higher alcohol to diesel fuel resulted in a decrease in NO_X, CO and unburned HC and smoke emissions and an increase in CO_2. NO_X, CO and unburned HC values of higher alcohol blended fuels at full load showed lower results, between 3.04–22.24%, 22.85–56.35% and 5.44–22.83%, respectively, compared to diesel fuel. It can be concluded that the use of hemp seed oil biodiesel and higher alcohol in the diesel engine will make a significant contribution to the reduction of NO_X emissions.

Keywords: Long-chain alcohol, Hempseed, Engine performance, Exhaust emission, Combustion characteristics.

Nomenclature

FFA	Free Fatty Acid
HSO	Hemp Seed Oil
HSOB	Hemp Seed Oil Biodiesel
D100	100% diesel (by vol.)
B20	80% diesel + 20% biodiesel (by vol.)
B20Pe10	70% diesel + 20% biodiesel + 10% pentanol (by vol.)
B20Pe20	60% diesel + 20% biodiesel + 20% pentanol (by vol.)
B20Pe30	50% diesel + 20% biodiesel + 30% pentanol (by vol.)
B20Hx10	70% diesel) + 20% biodiesel + 10% hexanol (by vol.)
B20Hx20	60% diesel + 20% biodiesel + 20% hexanol (by vol.)

* Corresponding authors: zeki.yilbasi@bozok.edu.tr, kadir.yesilyurt@bozok.edu.tr

B20Hx30	50% diesel + 20% biodiesel + 30% hexanol (by vol.)
B20Hp10	70% diesel + 20% biodiesel + 10% heptanol (by vol.)
B20Hp20	60% diesel + 20% biodiesel + 20% heptanol (by vol.)
B20Hp30	50% diesel + 20% biodiesel + 30% heptanol (by vol.)
CO	Carbon monoxide
CO_2	Carbon dioxide
O_2	Oxygen
NO_X	Nitrogen oxides
HC	Hydrocarbon
BTE	Brake Thermal Efficiency
KOH	Potassium Hydroxide
P_e	Brake power
BSFC	Brake Specific Fuel Consumption
BSEC	Brake Specific Energy Consumption
LHV	Lower Heating Value
T	Brake torque
$\dot{m}_f$	Fuel mass flow rate
Q	Energy supplied from the fuel
n	Engine speed
HRR	Heat Release Rate
V	Cylinder volume
θ	Crank angle
P	Cylinder pressure
EGT	Exhaust Gas Temperature
CP	In-cylinder gas pressure
SOI	Start of Injection
CHR	Cumulative Heat Release
CHR_m	Maximum Cumulative Heat Release
ID	Ignition Delay
SOC	Start of combustion
EOC	End of Combustion
MGT	Mean Gas Temperature
FLP	Fuel Line Pressure
BMEP	Brake Mean Effective Pressure
CP_m	Maximum in-cylinder gas pressure
HRR_m	Maximum Rate of Heat Release
MGT_m	Maximum Mean Gas Temperature
TDC	Top Dead Center

1 Introduction

Energy is one of the most basic needs required to sustain any activity in daily life. Therefore, a consistent and sustainable energy supply with security and accessibility is essential for the development of countries. Nevertheless, the use of energy and energy demand have been increasing rapidly all over the world due to technological progress, industrialization, increasing population and improvements in people's living standards since the 21st century [1]. Especially in developing countries, the energy demand part of this problem is increasing with the socio-economic rise. In fact, oil consumption increased by approximately 1.5% (1.4 million barrels on average) per day in 2018, which could be met by increasing global oil production by an average of 2.2 million barrels per day [2].

Internal combustion engines (especially compression ignition engines) using significant amounts of petroleum-based fuels play an important role in many sectors such as agriculture, transportation and energy generation [3, 4]. With the advancement of technology in these sectors, it can be estimated that there is a similar increase in the number of vehicles using diesel fuel. In parallel with this increase, the need for renewable and sustainable fuels that can be diesel substitutes comes to the forefront due to environmental problems, high cost and continuous consumption of petroleum-based diesel fuels. In other words, the previously mentioned reasons accelerated the transition to alternative fuels that can be used instead of petroleum-based diesel fuels [5–7]. Consequently, many alternative fuels such as vegetable oils, biodiesel, alcohol, natural gas, ethers [8], and Fischer-Tropsch diesel [9] have attracted the attention of researchers. Vegetable oils, which are listed among these alternatives, cannot be used directly in a diesel engine as an energy source since they cause difficulty in starting in cold weather, clogging of filters, pipes and injectors, and knocking in the short term due to their high viscosity, low cetane number, low flash point, natural gums, low volatility and reactivity of unsaturated hydrocarbon chains in their presence, and they cause carbon deposits on pistons and engine head, excessive engine wear and deterioration of engine lubricating oil due to polymerization in the long run [10, 11]. Furthermore, the reasons such as Free Fatty Acid (FFA) content significantly limit their use. Biodiesel is produced from vegetable oils by overcoming these disadvantages by the methods such as dilution, microemulsion formation, pyrolysis and transesterification [12]. Therefore, biodiesel comes into the forefront as an alternative fuel and additive for diesel engines [13].

Most of the biodiesel, which can be produced from various raw materials, originates from vegetable oil. Plants have a very important place in the ecosystem. Cereals constitute 80% of the global food supply [14]. The fact that a large part of such vegetable oil sources is of food quality brings along food and fuel conflicts. Nowadays, the fact that approximately 95% of the global annual production of biodiesel consists of edible oils causes serious effects on food supply [15]. Hemp Seed Oil (HSO) is mainly used in non-food products. Furthermore, the hemp plant grows relatively quickly, depending on the purpose, planting time, planting type and climatic conditions. Therefore, a sufficiently large quantity of hemp seeds can be produced under certain growing conditions for HSO production. In general, it is reported that hemp seeds have a fixed oil content ranging from 25% to 35% [16]. So, HSO can be considered as a raw material that can be preferred in biodiesel production.

As a result of the combustion of fuels used in diesel engines, many parameters may affect the emission amount of diesel engines due to combustion, which is a complex process [17]. Incomplete combustion of fuels caused by the lack of oxygen is one of the main sources of diesel engine emissions. The additives containing oxygen may help to eliminate this problem. The fuel blends created by increasing the oxygen ratio in the fuel are an important solution method to overcome the incomplete combustion problem. Alcohols are one of the most commonly used types of oxygen additives. Alcohols can be used by blending with diesel or biodiesel fuel or by adding them to the diesel–biodiesel blend [18]. The alcohols used can be low carbon number such as methanol and ethanol or high carbon number such as pentanol, hexanol and heptanol.

Compared to widely studied low-carbon alcohols such as ethanol, methanol and butanol, pentanol is a 5-carbon alcohol with the potential to be blended with diesel fuel due to its higher cetane number, higher energy density, less hygroscopic nature, and better mixing stability [19]. Some properties of pentanol such as viscosity, density and latent heat of vaporization are closer to diesel fuel than other alcohols. Hexanol, a seven-carbon alcohol, has great potential compared to short-chain alcohols due to its latent heat of vaporization, density, viscosity, high energy density and cetane number, as well as good blending stability with diesel fuel [20, 21]. Furthermore, hexanol is used to improve the combustion and physicochemical properties of diesel–biodiesel mixtures [22]. Hexanol can be used in ternary blends, especially in low-carbon alcohol–biodiesel–diesel mixtures, which lack self-ignition properties, have lower heat release capacity and lower energy content due to their high viscosity, as an ignition improver or oxygen additive [23, 24]. Heptanol is an alcohol with fuel properties similar to fossil-based diesel fuel [25–27]. Heptanol has started to be considered as a potential non-fossil fuel substitute for diesel engines with the discovery of new production methods such as using microbial pathways [28, 29]. Heptanol is known to have higher energy content, cetane number and flash point than alcohols with carbon number 1–6, as well as physicochemical properties such as lower oxygen content and more auto-ignition temperature [30, 31]. There is a limited number of studies on heptanol combustion reaction kinetics and mechanisms [32]. The combustion behavior is improved with the use of heptanol depending on the oxygen content [27]. The addition of heptanol to diesel fuel increases the maximum in-cylinder gas pressure (CP) and prolongs the ignition delay [33].

As a result of the study conducted by Pandian *et al.* [34], the addition of 10% and 20% hexanol by volume to cashew nut biodiesel provided a reduction in harmful pollutants. Furthermore, a remarkable enhancement in Brake Thermal Efficiency (BTE) and a diminishment in brake specific fuel consumption (BSFC) were achieved. In their study, John and Raja [35] discussed the suitability of hemp biodiesel obtained from non-edible industrial hemp (*Cannabis sativa* L.) seed oil as a biofuel in diesel engines. In terms of emissions, B10 emitted less NO_X (440 ppm), B50 emitted less CO emissions (16%), B30 emitted less HC emissions (48 ppm) and B10 emitted less smoke emissions (76.40) at the highest load conditions. The hemp biofuel blends also resulted in reductions of CO and HC emissions by 20.83% and 24.5% at peak load. In terms of combustion characteristics, CP of B50 is greater than that of diesel fuel, showing that B30 has a maximum heat release rate (HRR) of 47.8 J/°CA. In their study, Sridhar *et al.* [36] investigated the effects of higher alcohol (1-pentanol) addition on engine performance and emission characteristics and reported that pentanol/diesel blends reduced the NO_X, HC and CO emissions compared to diesel fuel, while there was a slight decrease in BTE in 1-pentanol/diesel blends. Pentanol/biodiesel blends also caused a slight reduction in BTE and reduced NO_X, HC and CO emissions compared to biodiesel. In their study, Nour *et al.* [22] investigated the influence of hexanol-diesel blends (10%, 20%, 30%, 40% and 50% by volume) on the combustion, performance and emission characteristics of a diesel engine. The results revealed that the addition of hexanol to diesel increased the ignition delay, improved the premixed combustion mode and inhibited the diffusion combustion mode. Furthermore, the total Cumulative Heat Release (CHR) for the Hex50 blend (50% hexanol and 50% diesel) increased by 9% and 4% at 75% and 100% engine loads, respectively. Nevertheless, BTE obtained for diesel fuel was 0.6% higher than for hexanol-diesel blends. BSFC of Hex50 mixture at 100% engine load was 6.4% higher than diesel. NO_X emissions and smoke opacity were reduced by 26% and 54%, respectively, for the Hex50 at 100% engine load. In their study, Pardo *et al.* [37] investigated the performance and emission characteristics of conventional diesel fuel by blending heptanol with 4% (HP4), 8% (HP8) and 16% (HP16) ratios. The results showed that the percentage of heptanol caused an increase in the maximum values of the pressure in the combustion chamber and the HRR. In general, the addition of heptanol to conventional diesel resulted in a 3.9% and 4.8% increase in the maximum values of these parameters. Furthermore, HP4, HP8 and HP16 heptanol blends reduced CO_2, NO_X and smog emissions by 11.7%, 6.7% and 37.1%, respectively.

Based on the results of previous studies, it can be concluded that ternary blends created by adding biodiesel and alcohol to diesel fuel can be a substitute for diesel fuel to reduce fossil fuel dependence, and even be beneficial in terms of some emissions. The main aim of this study was to fuel a diesel engine with ternary fuels consisting of diesel, biodiesel (HSOB) and higher alcohols (pentanol, hexanol and heptanol) for four different engine loads (25%, 50%, 75% and 100%) and to evaluate the combustion, emission and performance characteristics. Furthermore, it was aimed to compare the results obtained from these fuels with the reference fuels diesel (D100) and B20 (80% diesel and 20% HSOB). In review of the literature, although there were studies on higher alcohols added to diesel–biodiesel blends at different rates, no experimental study in which three different higher alcohols such as pentanol (Pe), hexanol (Hx) and heptanol (Hp) were evaluated comparatively was found. With this strategic understanding, nine ternary blends including B20Pe10 (70% diesel, 20% biodiesel, 10% pentanol), B20Pe20 (60% diesel, 20% biodiesel, 20% pentanol), B20Pe30 (50% diesel, 20% biodiesel, 30% pentanol), B20Hx10 (70% diesel, 20% biodiesel, 10% hexanol), B20Hx20 (60% diesel, 20% biodiesel, 20% hexanol), B20Hx30 (50% diesel, 20% biodiesel, 30% hexanol), B20Hp10 (70% diesel, 20% biodiesel, 10% heptanol), B20Hp20 (60% diesel, 20% biodiesel, 20% heptanol), and

B20Hp30 (50% diesel, 20% biodiesel, 30% heptanol were prepared. The combustion, emission and performance characteristics of the above blends were compared with D100 (diesel fuel) and B20 (80% diesel fuel, 20% biodiesel) and also discussed with the other relevant studies.

2 Materials and methods

2.1 Materials

In this study, industrial hemp (*Cannabis sativa* L.) seeds, which are the raw material of vegetable oil used in biodiesel production, were obtained from a commercial enterprise located in Konya, Turkey. Baseline diesel fuel, whose technical properties meet EN 590 standard, was purchased from a local station in Yozgat, Turkey. *Merck* (Darmstadt, Germany) brand methanol (CH_3OH) with a molecular weight of 32.04 g/mol and a purity of 99.9% was used to produce biodiesel from industrial hemp-*Cannabis sativa* L. seed oil. *Tekkim* (Bursa, Turkey) brand potassium hydroxide (KOH) with a molecular weight of 56.11 g/mol and a purity of ≥90% was preferred as catalyst in the reaction. While *Acros Organics* (NJ, USA) brand was preferred for pentanol (≥99% purity) used as fuel additive, *Merck* (Darmstadt, Germany) brand preferred was preferred for hexanol (≥98% purity), and *Merck* (Darmstadt, Germany) brand was preferred for heptanol. The In the selection of the above materials, those in the inventory were used first, and if there was none, the material that was easy to supply was selected.

2.2 Preparation of HSOB

HSO, which is used in biodiesel production, was obtained from hemp seeds using a screw cold-pressed oil extraction press located in the test area of *General Makina ve Mühendislik* (Ankara, Turkey). As a result of the pressing and filtering process of hemp seeds, 25% crude oil was obtained. Before starting the transesterification process, FFA content was investigated and found to be 1.75% in order to decide whether the transesterification process would be one-stage or two-stage. Because this value was below 2%, a one-step reaction was chosen [38]. In this study, the Taguchi approach was preferred since it is a multivariate statistical technique that helps to comprehend the interactions of catalyst amount, alcohol to oil molar ratio, reaction temperature and reaction time parameters, and allows the selection of the most suitable variables to predict the maximum biodiesel yield, economically, thanks to an insufficient number of experiments and minimal source consumption [39]. In our previous study, optimization of transesterification parameters using the Taguchi method and HSOB produced under optimum conditions were mentioned in detail [40]. In this context, catalyst concentration of 0.9%, molar ratio of 12:1 methanol to oil, reaction temperature of 45 °C and reaction time of 120 min were determined as optimum transesterification reaction conditions.

The transesterification process was started by filling the HSO into a clean beaker. The HSO sample was heated to 130 °C for 2 h to evaporate excess water droplets that may be present in the oil and also to reduce the viscosity of the oil [41]. Since the density of HSO is reduced due to this process, suspended carbon particles could be easily removed with a fine cloth filter with a pore size of 0.1 mm. Then, impurities that may be present in HSO content were removed by filtering through qualitative filter paper before being used in biodiesel production. Methoxide solution was obtained by dissolving all of the KOH in the closed glass bottle in methanol with the above-mentioned amount of KOH and methanol using the shake-mix method. The reaction was performed in a 2000 mL flask with a reflux condenser and a thermometer (to monitor the temperature of the reaction) on a *Scilogex* brand MS7-H550-Pro magnetic stirrer. HSO was taken into the reaction flask at the prescribed rate. The heated magnetic stirrer was raised to this temperature to carry out the transesterification reaction at a constant temperature of 45 °C. A stirring speed of 1250 rpm was selected from the magnetic stirrer panel and all experiments were carried out at this speed. When the temperature of the HSO reached the desired level, the methanol-KOH solution was transferred to the reaction flask with the help of a funnel and the reaction was started. After 120 min, the reaction was stopped. The sample in the reaction flask was taken to a separating funnel and left to rest for 8 h in order for the glycerol to sink due to the separation of the sample due to the density difference and the effect of gravity. The underlying glycerol and other impurities were discharged into a vessel with a drain valve in the separating funnel. Afterward, the methyl ester was poured into a beaker and kept for 1 h at a constant temperature of 70 °C to remove the unreacted methanol in its content. Afterwards, the temperature of the crude HSOB was taken to the separating funnel to carry out the purification process, and its temperature was expected to decrease to 55 °C. The biodiesel was washed by spraying on distilled water at the same temperature (55 °C) until it became neutral and left for 12 h. Waste water and other substances (unreacted methanol, catalyst and other impurities) in the separating funnel were removed with the help of the drain valve. Then, the washed methyl ester was poured into a beaker and dewatered by heating at 120 °C for 2 h. Biodiesel was kept waited in a screw cap glass bottle until it decreased to ambient temperature. Finally, the mass of the biodiesel sample was measured using a precision balance and the biodiesel yield was calculated [38, 42]. As a result of this calculation, the final yield of biodiesel produced from HSO was found to be 96.19.

QP2010 model Gas Chromatography (GC) system of Shimadzu brand equipped with RXI-5MS capillary column (30 m × 0.25 mm) was used to analyze the fatty acid profiles of HSO and its biodiesel. The fatty acid components of HSO and the biodiesel produced from it are presented in Table 1. In conclusion, the highest unsaturated fatty acid content was determined in linoleic acid (55.44% and 55.40%) and linolenic acid (17.91% and 17.84%) for both vegetable oil and biodiesel. Palmitic acid (6.52% and 6.51%) is at the top of the list of saturated fatty acids.

Basic fuel characteristics of petroleum-based diesel fuel, biodiesel and higher alcohols (pentanol, hexanol and heptanol) used in the experiments are presented in Table 2.

Table 1. Fatty acid profile of HSO and biodiesel produced from it.

Fatty acid	Formula	Structure	HSO (%)	HSOB (%)
Palmitic	$C_{16}H_{32}O_2$	16:0	6.52	6.51
Palmitoleic	$C_{16}H_{30}O_2$	16:1	0.07	0.07
Stearic	$C_{18}H_{36}O_2$	18:0	2.81	2.84
Oleic	$C_{18}H_{34}O_2$	18:1	15.25	15.30
Elaidic	$C_{18}H_{34}O_2$	18:1	0.75	0.78
Linoleic	$C_{18}H_{32}O_2$	18:2	55.44	55.40
Linolelaidic	$C_{18}H_{32}O_2$	18:2	0.34	0.33
Linolenic	$C_{18}H_{30}O_2$	18:3	17.91	17.84
Arachidic	$C_{20}H_{40}O_2$	20:0	0.36	0.38
Gondoic	$C_{20}H_{38}O_2$	20:1	0.15	0.15
Behenic	$C_{22}H_{44}O_2$	22:0	0.23	0.24
Erucic	$C_{22}H_{42}O_2$	22:1	0.07	0.08
Lignoceric	$C_{24}H_{48}O_2$	24:0	0.09	0.09

Table 2. Properties of the fuels used in the tests [19, 33, 43–45].

Fuel properties	Diesel	HSOB	Pentanol	Hexanol	Heptanol
Chemical formula	$C_{14}H_{25}$	$C_{17.60}H_{30.47}O_2$	$C_5H_{12}O$	$C_6H_{14}O$	$C_7H_{16}O$
Molecular weight (g/mol)	193	273.72	88.15	102.18	116.20
Density at 15 °C (kg/m^3)	823	875	814.8	821.8	818
Kinematic viscosity at 40 °C (mm^2/s)	2.65	3.429	2.89	3.64	3.32
Calorific value (MJ/kg)	43.85	38.737	32.16	39.10	39.92
Cetane number	53.5	36.5	20	23	29.5
Flash point (°C)	59	>120	49	59	76
Carbon (wt. %)	87.05	77.18	68.13	70.52	72.16
Hydrogen (wt. %)	12.95	11.13	13.61	13.74	13.71
Oxygen (wt. %)	0	11.69	18.26	15.74	14.13
Carbon/Hydrogen	6.72	6.93	5.01	5.13	5.26
Latent heat of evaporation (kJ/kg)	275	240	308.05	486.00	574.95

2.3 Formation of triple fuels consisting of diesel fuel, biodiesel and higher alcohols

In this experimental study, nine different fuel blends and diesel and biodiesel fuel as reference fuel were tested to investigate the engine performance, exhaust emissions and combustion characteristics of a compression ignition engine. During the determination of the blending ratios of the test fuels, it was determined that two types of blending ratios, generally B20 (80% diesel – 20% biodiesel) and B2 (98% diesel – 2% biodiesel) for biodiesel–diesel blends, came to the forefront [46]. B2 is used because it improves the properties of the lubricating oil used in diesel engines. B20 was preferred in this study since B2 has the feature of reducing exhaust emissions as well as this property [47]. Therefore, HSOB was first prepared by blending 80% petroleum-based diesel fuel with 20% biodiesel, and this binary blend was labeled as B20. Then, a ternary fuel blend of 20% biodiesel, 10%, 20% and 30% higher alcohol (pentanol, hexanol and heptanol) and diesel fuel (50%, 60% and 70%) by volume, respectively, was formed. In other words, the ternary fuel samples obtained were as follows: B20Pe10 (20% biodiesel + 70% diesel fuel + 10% pentanol), B20Pe20 (20% biodiesel + 60% diesel fuel + 20% pentanol), B20Pe30 (20% biodiesel + 50% diesel fuel + 30% pentanol, B20Hx10 (20% biodiesel + 70% diesel fuel + 10% hexanol), B20Hx20 (20% biodiesel + 60% diesel fuel + 20% hexanol), B20Hx30 (20% biodiesel + 50% diesel fuel + 30% hexanol), B20Hp10 (20% biodiesel + 70% diesel fuel + 10% heptanol), B20Hp20 (20% biodiesel + 60% diesel fuel + 20% heptanol), and B20Hp30 (20% biodiesel + 50% diesel fuel + 30% heptanol). The splash mixing technique was preferred since it is an inexpensive and useful technique for the preparation of fuel blends to be tested in a diesel engine. Then, the ternary blends were kept in the dark for a week to observe whether the problem of phase separation would occur. All ternary test fuels were checked for phase separation prior to use in the test engine and were found to show

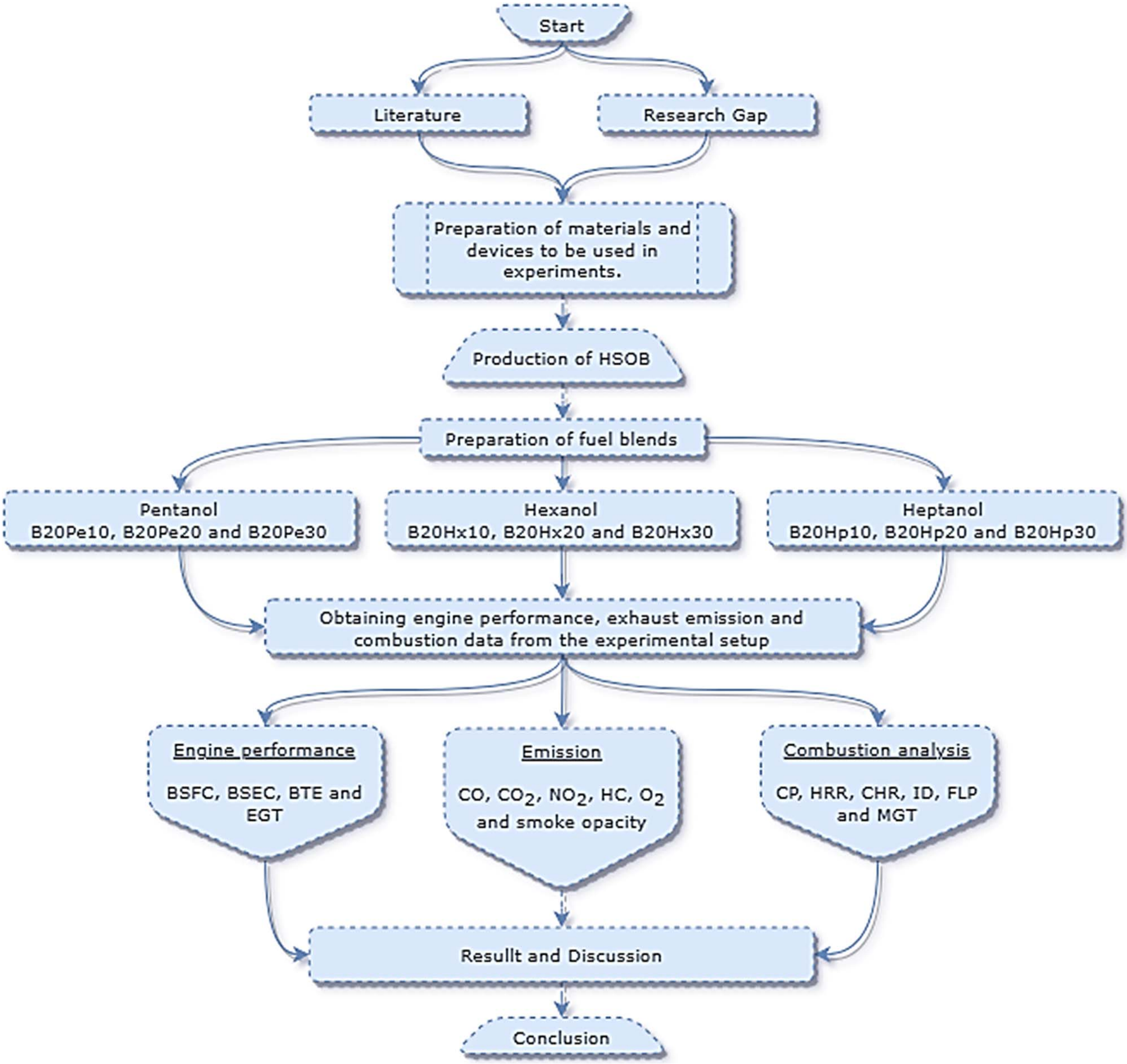

Figure 1. The flowchart showing each step in the study from the beginning to the end.

no phase separation. The flowchart showing each step in the study from the beginning to the end is presented in Figure 1.

2.4 The experimental setup

In this experimental study, engine parameters including performance, emission and combustion characteristics were tested in the engine test setup in Kırıkkale University, Kırıkkale Vocational School, Automotive Technology Laboratory. Test fuels were tested in a *Kirloskar* brand TV1 model, 4-stroke, single-cylinder, water-cooled, atmospheric, and direct injection test engine. The technical specifications of the test engine used are presented in Table 3. An air-cooled *Galen-Tech* brand active dynamometer and load cell with data in the range of 0–5000 rpm were used for the torque measurements of the experimental engine. There is a *Siemens brand* Sinamics G120 PM250 model load cell on the dynamometer. The experiments were carried out at a constant engine speed of 1500 rpm for each test fuel. EJA110E-JMS5J-912NN model of Yokogawa brand (calibration range 0–500 mmH_2O, output linear) integrated with ICEngineSoft engine performance analysis software, electronic fuel monitoring system and a data collection system DAQ (16-bit DAQ, NI-USB-6210) transmitted the information collected from different sensors to the computer to which it was connected *via* a USB interface. *Apex* brand (glass) FF0.012 model fuel metering unit was used. Air consumption was measured using the SL-1-A-MQA-ND-ZA4Z-ZZZ model (output 4–20 mA, supply 10–30 V dc,

Table 3. Detailed specifications of the test engine.

Engine supplier	*Apex Innovations Pvt. Ltd.*
Brand and model	*Kirloskar* TV1
Rated power	5.2 kW
Speed	1500 rpm
Number of strokes per cycle	4
Number of cylinders	1
Valve system	2 valves per cylinder
Fuel injection type	Direct injection
Stroke	110 mm
Bore	87.50 mm
Cooling system	Water cooled
Swept volume	661.45 cm^3
Intake system	Naturally aspirated
Injector nozzle number	4
Compression ratio	18/1
Fuel injection timing	23 °CA before TDC
Nozzle opening pressure	200 bar
Opening advance of intake valve	4.5 °CA before TDC
Closing delay of intake valve	35.5 °CA after TDC
Opening advance of exhaust valve	35.5 °CA before TDC
Closing delay of exhaust valve	4.5 °CA after TDC
Fuel tank capacity	15 L

connection 1/2″ NPT(M), range (–)25–0 mbar) air flow velocity meter of *WIKA* brand. DAQ (16-bit DAQ, NI-USB-6210), a data collection system integrated with ICEngineSoft engine performance analysis software, transmitted the information collected from different sensors to the computer it is connected to *via* a USB interface. Abustek brand Fr Block model, K-type thermocouples that can measure temperatures between 0–1200 °C and Pt100 type thermocouples that can measure temperatures between 0–100 °C were used to measure exhaust gas, engine coolant and calorimeter inlet–outlet temperatures on test equipment. *PCB Piezotronics* brand S111A22 model diaphragm stainless steel type and hermetically sealed pressure sensor with 5000 psi measuring range and 1 mV/psi sensitivity was used to determine the combustion characteristics of the test engine. Furthermore, the environmental noise effect on the signals was minimized by using a low noise cable. A 8.KIS40.1361.0360 model crank angle encoder of *Kubler* brand was installed to measure the crankshaft position at every 1 degree. Other combustion parameters such as crank angle and CP, HRR, and ignition delay time obtained from the tests performed for each fuel type at different engine loads (25%, 50%, 75% and 100%) with the NI-USB-6210 data acquisition system were collected and recorded.

Bilsa brand MOD 2210 model exhaust gas emission device with a detection time of less than 5 s was used for the measurement of exhaust emissions. The measurements of carbon monoxide (CO) and carbon dioxide (CO_2) with 0.001% accuracy, unburned hydrocarbon (HC) and nitrogen oxide (NO_X) with 1% accuracy, and oxygen (O_2) emissions with 0.01% accuracy can be performed with this device. BEA 350 model device of Bosch brand, which can measure with 1% accuracy, was used for smoke opacity measurements.

2.5 Test methodology

The experimental setup to determine the engine performance, exhaust emissions and combustion characteristics of the prepared fuels was constituted of (i) engine test system for measurements of engine torque, fuel and air consumptions, engine coolant temperature (inlet and outlet temperatures) and Exhaust Gas Temperature (EGT), (ii) exhaust emission measurement set for measurements of unburned HC, O_2, CO, NO_X, CO_2, and smoke opacity emissions, and (iii) CP measurement system for in-cylinder combustion analysis. The engine test setup diagram is presented in Figure 2.

Before starting the tests, the engine oil was changed and the coolant assembly was checked. Then, the calibration processes were completed. Afterwards, preliminary tests were performed at 18:1 compression ratio, 1500 rpm constant speed and variable loading conditions (25%, 50%, 75%, and 100%) to monitor operating conditions of diesel engine [48]. With an active current dynamometer, engine tests were performed with 3.7 kg, 7.4 kg, 11.1 kg, and 14.8 kg steps for 25%, 50%, 75%, and 100% loads, respectively. The tests were performed at 1500 rpm engine speed

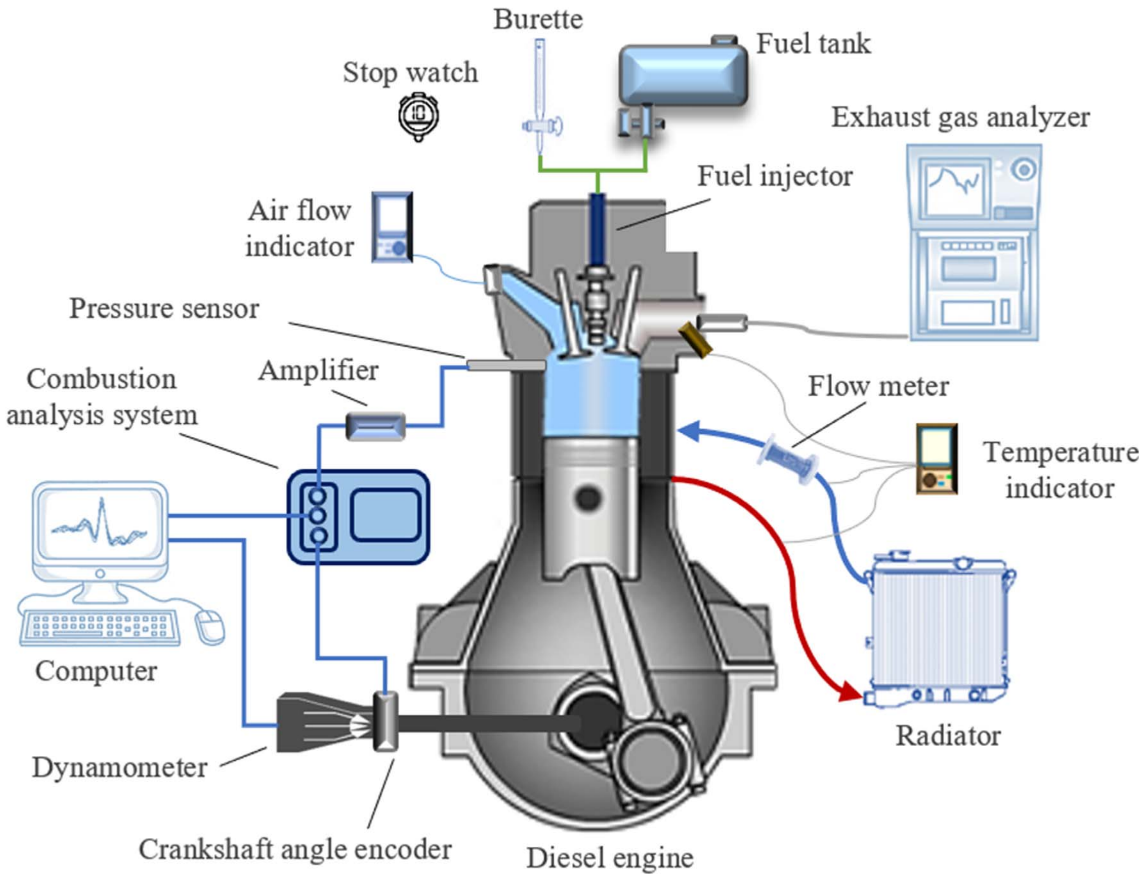

Figure 2. Schematic diagram of the test engine and other equipment.

fixed by the experimental set software and at four different engine loads. Each experiment was repeated three times and the averages of the obtained results were taken into account. The braking power (Pe), BSFC, BSEC, and BTE values of all fuels at different engine loads were calculated by equations (1)–(4) using the data obtained from the experiments:

$$P_e = (2 \cdot \pi \cdot T \cdot n)/(60 \cdot 10^3), \tag{1}$$

$$\text{BSFC} = \dot{m}_f / P_e, \tag{2}$$

$$\text{BSEC} = (\dot{m}_f \cdot \text{LHV})/P_e, \tag{3}$$

$$\text{BTE} = P_e / Q, \tag{4}$$

where T represents the engine torque, n represents the engine speed, $\dot{m}_f$ represents the mass flow rate of the tested fuel, LHV represents the lower heating value of the fuel and Q represents the energy supplied from the tested fuel.

Before starting the emission measurement, the calibration processes of the exhaust emission test device and the smoke density meter were carried out. The results of each test were noted when the engine was stabilized. Then the HC, NO_X, CO, CO_2 and O_2 exhaust emissions were converted to g/kW h according to the following conversion procedure:

$$\text{HC}\,(\text{g}/kW\ \text{h}) = 2.002 \cdot 10^{-3} \cdot \text{HC}\,(\text{ppm}), \tag{5}$$

$$\text{NO}_\text{x}(\text{g}/kW\ \text{h}) = 6.636 \cdot 10^{-3} \cdot \text{NO}_\text{x}\,(\text{ppm}), \tag{6}$$

$$\text{CO}\,(\text{g}/kW\ \text{h}) = 3.591 \cdot 10^{-3} \cdot \text{CO}\,(\text{vol\%}), \tag{7}$$

$$\text{CO}_2\,(\text{g}/kW\ \text{h}) = 63.470 \cdot \text{CO}_2\,(\text{vol\%}), \tag{8}$$

$$\text{O}_2\,(\text{g}/kW\ \text{h}) = 41.024 \cdot \text{O}_2\,(\text{vol\%}). \tag{9}$$

The CP of the diesel engine under all engine loads was recorded at 1° crank angle intervals up to 720° crank angle in each working cycle. Average CP values, in which a filtering method was applied with at least 50 cycle records, were considered.

According to the first law of thermodynamics during combustion, the increase in internal energy depending on the crank angle and the net Heat Release Rate (HRR) converted into mechanical work were calculated using equation (10):

$$\frac{\text{d}Q_\text{net}}{\text{d}\theta} = \frac{k}{k-1} P \frac{\text{d}V}{\text{d}\theta} + \frac{1}{k-1} V \frac{\text{d}P}{\text{d}\theta}, \tag{10}$$

where; $\text{d}Q_\text{net}$ (J) represents the energy transferred to the wall of cylinder and the wall of combustion chamber at the completion of combustion, k represents the ratio of specific heats, P (Pa) represents CP, θ (°CA) represents the crank angle and V (m^3) represents the volume of cylinder.

Errors and uncertainties may arise due to various parameters such as calibration, environmental conditions, observation, reading, equipment selection and test planning [27, 49]. Uncertainty analysis measures the accuracy of the experiments performed [50]. In this thesis study, the uncertainty analysis was performed by taking into account the uncertainties of the devices used in the experiments in order to increase the accuracy of the results observed [51]. The square root technique proposed by Holman [52] was applied to calculate the uncertainties in the motor trials. Consequently, the load and velocity uncertainty of pressure sensor, encoder, CO, CO_2, HC, NO_X, opacity, temperature, burette system, stopwatch, and manometer were found to be ±0.53%, ±1.0%, ±0.75%, ±0.64%, ±0.98%, ±0.92%, ±0.51%, ±0.72%, ±1.0%, ±0.2%, ±0.78%, ±0.83% and ±0.067%, respectively. Total uncertainty was calculated as ±2.72%, below the acceptable range of 5% [27]. In this context, the overall uncertainty of the system was within the reasonable limits.

3 Results and discussion

In this section, the tests were performed at a fixed speed of 1500 rpm and 4 different loads (25%, 50%, 75%, and 100%) using 11 different fuels (D100, B20, B20Pe10, B20Pe20, B20Pe30, B20Hx10, B20Hx20, B20Hx30, B20Hp10, B20Hp20 and B20Hp30), and the engine characteristic results (specific fuel and energy consumption, average effective pressure, effective thermal efficiency and EGT), exhaust emission (NO_X, CO_2, CO, HC, O_2 and smoke emission) and the combustion analysis results (HRR, CHR, fuel line pressure, pressure rise rate, average gas temperature, ignition delay) were investigated.

3.1 Engine characteristic results

Engine performance characteristics were investigated by evaluating BSFC, BSEC, BTE, and EGT. The investigated parameters were discussed in detail in the following subsections by taking into account the recent literature.

3.1.1 Brake specific fuel consumption

BSFC provides a comparison between the amount of fuel consumed at a given time and the power produced by the test engine. It is a very important criterion in the fuel selection of a diesel engine since it shows the fuel economy and efficiency [53]. When less fuel is consumed than a certain power level, the BSFC value is also expected to be lower. The specific fuel consumption of the fuel blends shows similar behavior and magnitude values as seen in Figure 3. It was seen that BSFC values decreased with the increase of motor load from 25% to 50%, 75% and 100%, respectively. While it was determined that there was a decrease of approximately 27.78% in the BSFC value when the load was increased from 25% load to 50% load the D100 fuel, which was taken as the reference fuel, there was a decrease of approximately 33.77% when the load was increased to 75%, and finally, there was a decrease of approximately 38.33% when the load was increased to 100%. In general, the main reason for this decrease for all fuels was the weak in-cylinder turbulence at low loads and the high inertia forces in the moving parts of the engine. However, with the increase in the engine load, the homogeneous distribution of the air/fuel blend in the cylinder, the improvement of the in-cylinder turbulence and the sufficient time required for combustion increased the combustion efficiency and this led to a decrease in the BSFC values [27].

When it was fueled with B20 fuel, it was seen that the increase in BSFC at each load increase was higher compared to D100 fuel. This can be explained by the increase in the amount of fuel consumed in order to maintain the same load situation, since the calorie of B20 fuel is lower. Furthermore, it was seen that it gave the highest BSFC values for all load values of B20Pe30 and B20Pe20 fuels, which are the lowest in the energy content ranking, supporting this explanation. It was also understood that the addition of pentanol to the B20 mixture increased the BSFC compared to other alcohol types. Since pentanol has lower cetane number, latent heat of vaporization and calorific value compared to hexanol and heptanol, it has a longer ignition delay and longer burning time, which worsens the combustion and has a negative impact on performance. BSFC values increase with the increase in alcohol content in mixtures containing alcohol. The fact that pentanol, hexanol and heptanol have lower calorific value and cetane number than diesel and hemp oil biodiesel increased the amount of fuel required to reach the same effective engine power at each engine load, and thus the BSFC. Furthermore, since the high latent heats of evaporation of alcohols will create a cooling effect, it is considered that alcohol-based fuels will evaporate more slowly and worsen the combustion, resulting in an increase in BSFC.

3.1.2 Brake specific energy consumption

The term, BSEC, is used to express the ratio of the energy obtained during one hour of fuel consumption to the unit effective engine power produced. The BSEC values of the fuel samples are directly related to the BSFC value. The BSEC graph of eleven different fuels tested in this study with engine load is presented in Figure 4. The decrease in BSEC values with the increase in motor load, seen in the figure, can be attributed to the decrease in thermal and mechanical energy losses in the total energy consumed [53, 54]. The decrease in the lower heating values due to the increase in the alcohol content in the ternary blends caused the BSEC to increase. The highest BSEC values for B20Pe30 and B20Pe20 fuels with the lowest lower calorific values were obtained at 25% load as 31.21 MJ/kW h and 28.69 MJ/kW h, respectively. At full load, the lowest BSEC values were calculated as 12.48 MJ/kW h, 13.06 MJ/kW h, 13.27 MJ/kW h, 13.35 MJ/kW h, 13.47 MJ/kW h and 13.59 MJ/kW h, respectively, for D100, B20, B20Hx10, B20Hp10, B20Hx20 and B20Pe10 fuels. It was thought that the higher cetane number led to a shortening of the ignition delay time, therefore, the fuels did not have time to blend with the air sufficiently, thus reducing the flammability

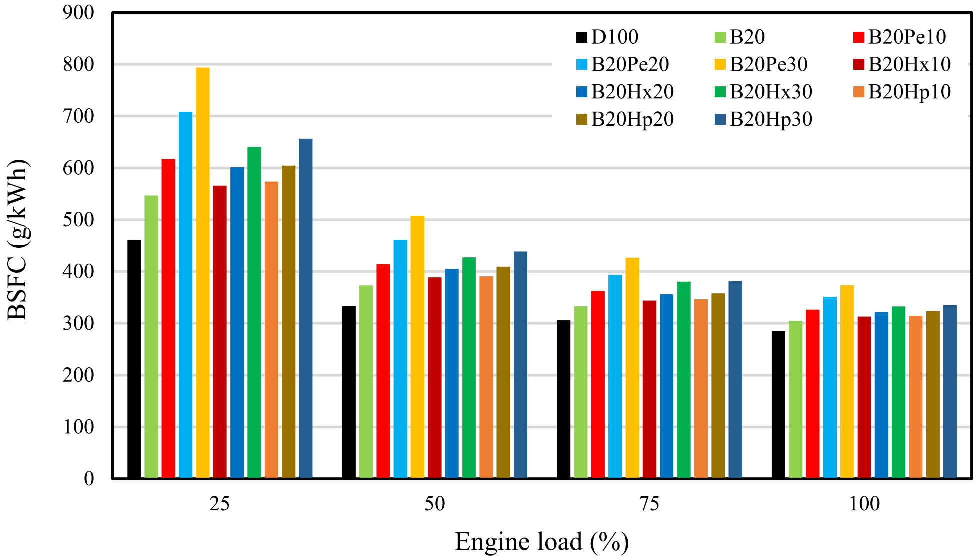

Figure 3. Variation of BSFC values depending on engine load.

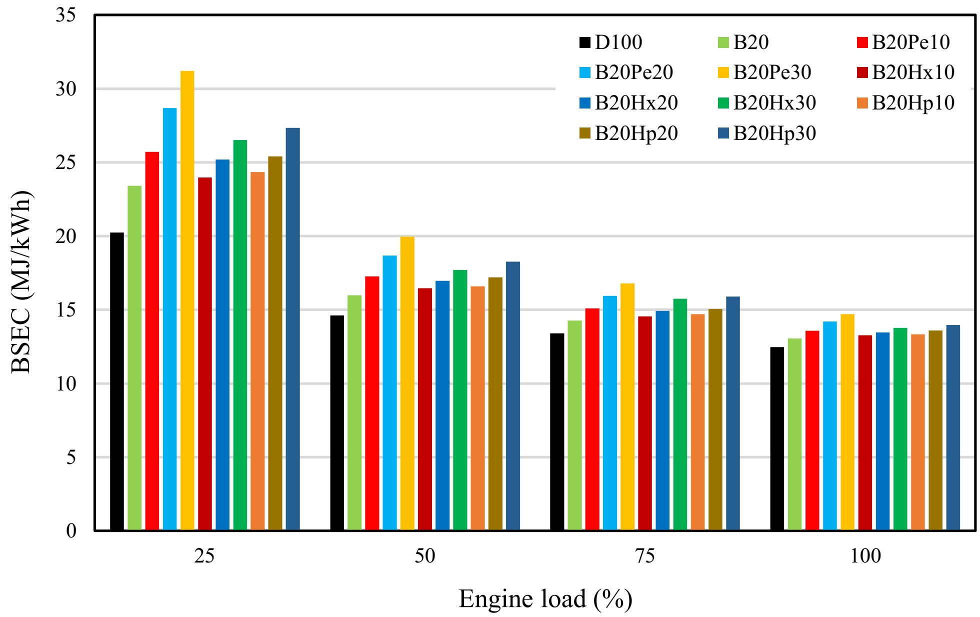

Figure 4. Variation of BSEC values depending on engine load.

due to the heterogeneous blend and thus increasing the energy requirement. Similar results were obtained in previous studies [55, 56].

3.1.3 Brake thermal efficiency

In internal combustion engines, the ratio of the effective engine power output data to the amount of thermal input provided by the fuel injected into the cylinder is expressed as the effective thermal efficiency (BTE) [57]. The highest BTE is achieved at the highest engine torque. The increase in combustion efficiency along with the increase in engine load and volumetric efficiency reduces BSFC and increases the engine torque [58, 59]. The change of BTE values depending on engine for all fuel samples tested is presented Figure 5. Among all fuels, D100 had the highest BTE values. It was thought that B20 fuel provided lower BTE values than D100 due to its lower calorific value as well as higher viscosity and density values. With the addition of pentanol, hexanol or heptanol to the B20 fuel, it was thought that the energy content of the fuel blends deteriorated and the BTE decreased due to the decrease in the heating values and cetane numbers of the fuels and the increase in the latent heat of evaporation. As the addition

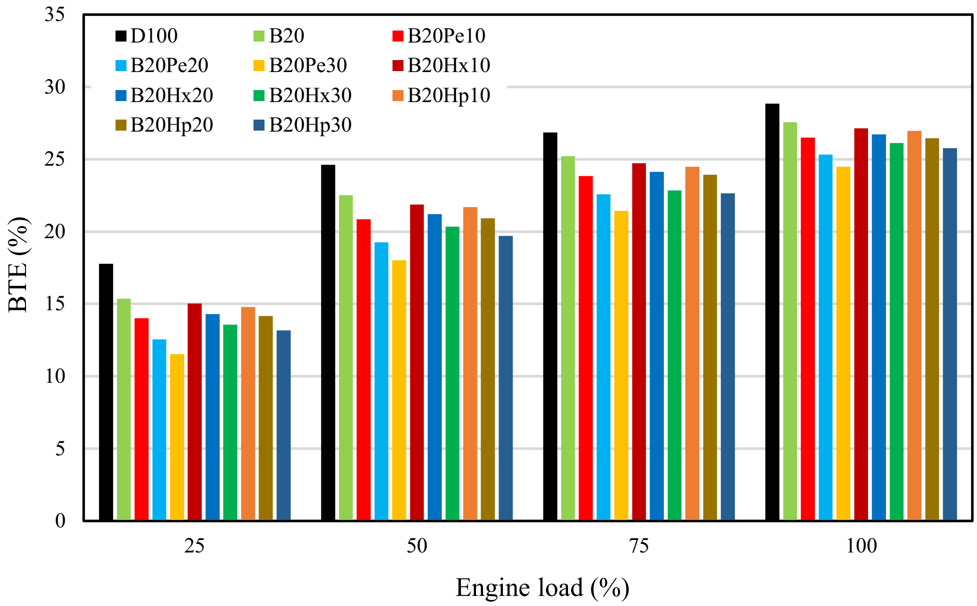

Figure 5. Variation of BTE values depending on engine load.

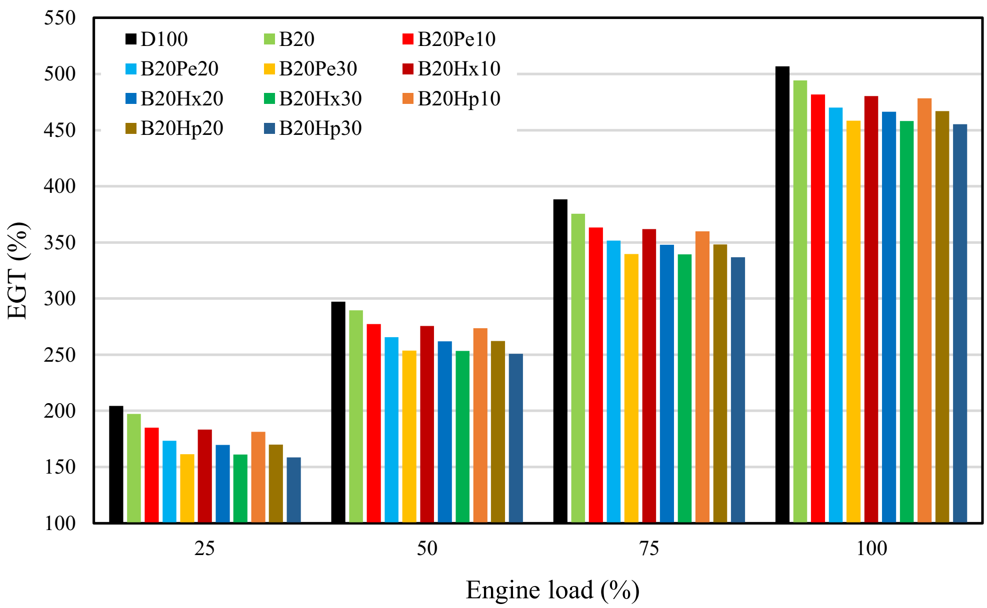

Figure 6. Variation of EGT values depending on engine load.

of alcohol increased, the BTE values decreased further due to the worsening of these properties of the fuel blends. Among the ternary blends containing alcohol, the highest BTE values were calculated as 27.14%, 26.97%, 26.73%, 26.49% and 26.46%, respectively, in B20Hx10, B20Hp10, B20Hx20, B20Pe10 and B20Hp20 fuels.

3.1.4 Exhaust Gas Temperature

EGT is a substantial parameter that gives an idea regarding the quality of the combustion process [60]. It is also a critical parameter in the change of emissions that constitute the exhaust gas content. The variation of EGT values of diesel, biodiesel and other ternary blend fuels according to engine load is presented in Figure 6. When the EGT values measured when diesel, biodiesel and ternary fuels containing alcohol were used were compared, it was seen that EGT values of ternary blends were lower than D100 and B20. When the EGT values were ranked from largest to smallest in fuels containing alcohol at full load, the values of 481.90 °C, 480.32 °C, 478.42 °C, 470.21 °C, 466.92 °C, 466.48 °C, 458.39 °C, 458.05 °C and 455, 42 °C, respectively, were measured for B20Pe10, B20Hx10, B20Hp10, B20Pe20, B20Hp20, B20Hx20, B20Pe30, B20Hx30 and

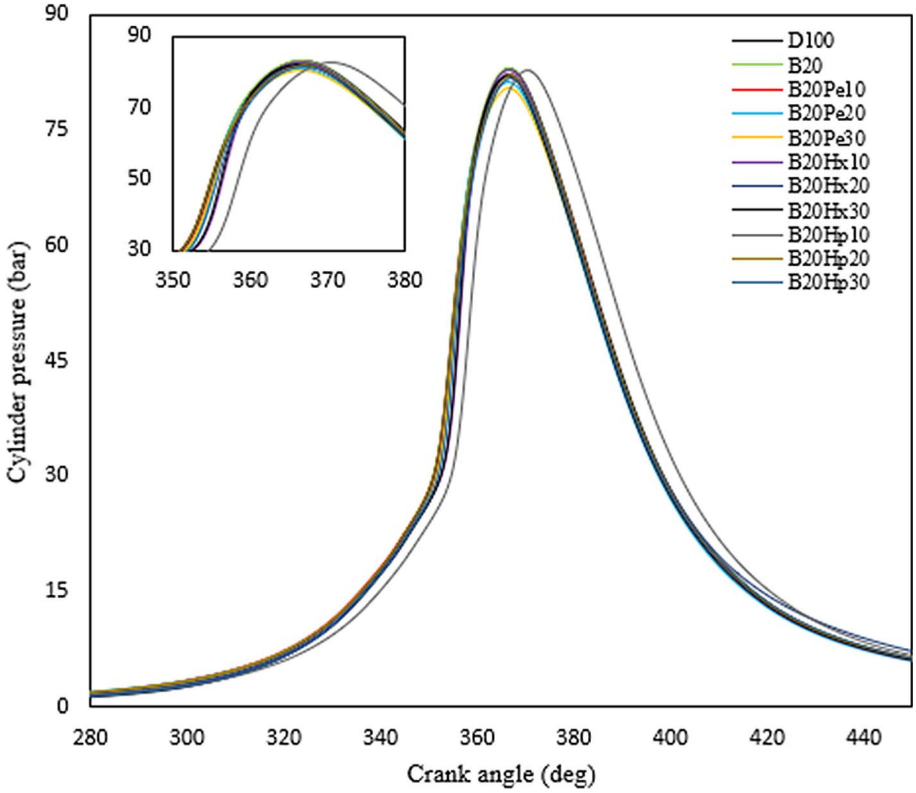

Figure 7. CP diagrams of test fuels at full load.

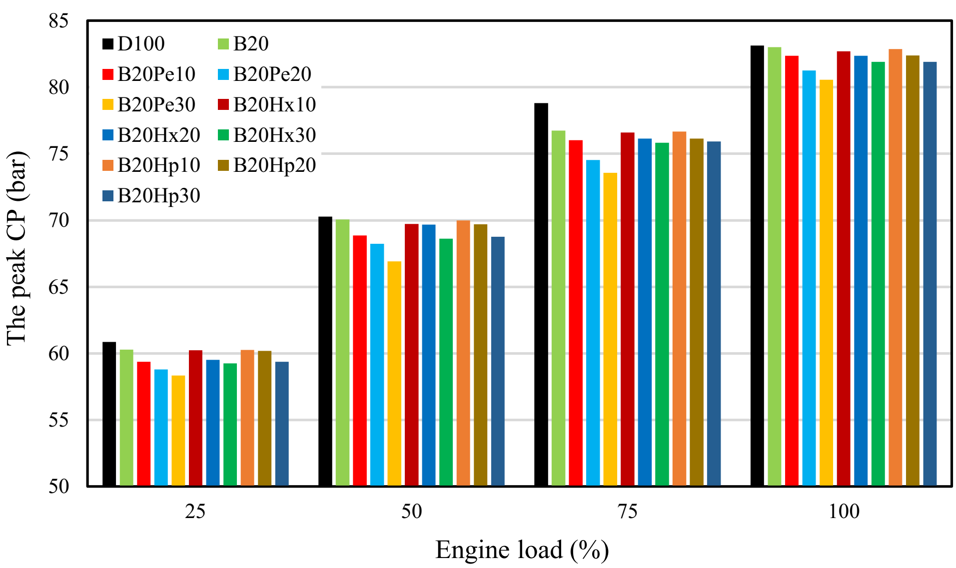

Figure 8. The peak CP variation as a function of engine load.

B20Hp30. All engine loads have a similar ranking. In this ranking, it was thought that the influence of the heating value was less, the effect of the latent heat of vaporization, oxygen content, and cetane number was more. As a result of the increased cooling effect of alcohols with the increase of alcohol content, it may be considered that the lowest EGTs occurred in fuel mixtures with 30% alcohol [19, 61].

3.2 Combustion analysis

The combustion characteristics were analyzed with the data created by measuring the CP at 25%, 50%, 75%, and 100% engine loads for all fuel samples tested. Extensive discussions on combustion characteristics are presented under this heading.

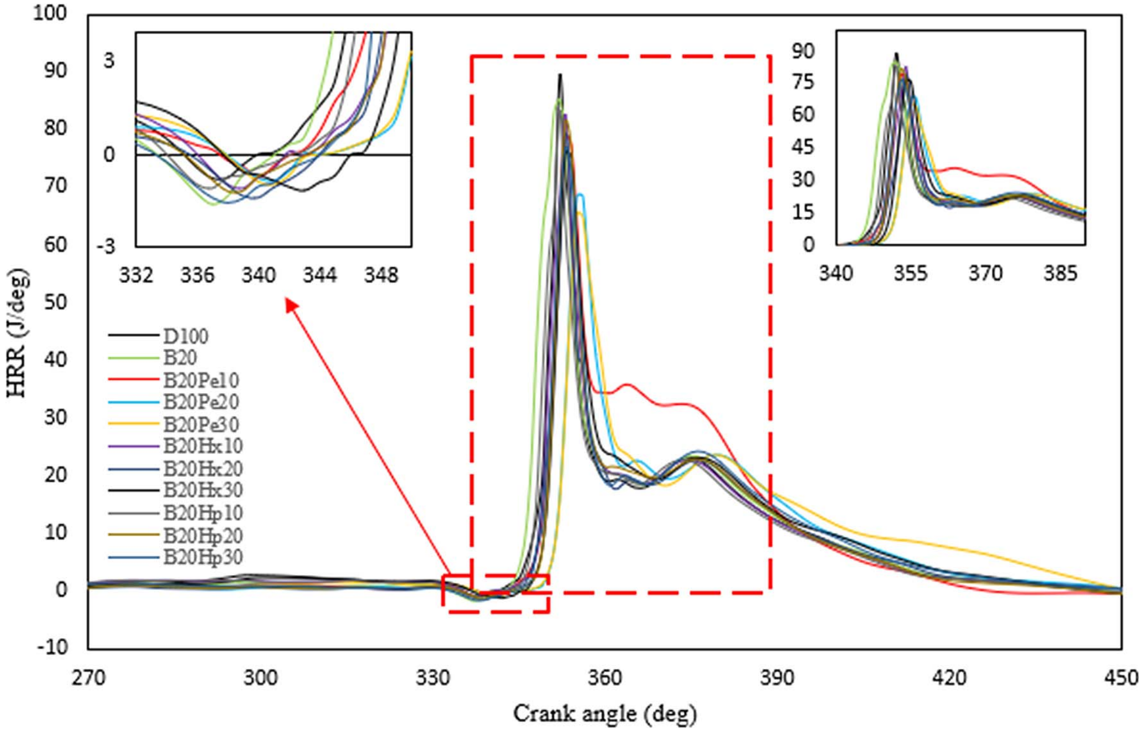

Figure 9. HRR diagrams of test fuels at full load.

3.2.1 In-cylinder gas pressure

Since CP is one of the most important parameters affecting the amount of conversion of chemical energy to braking power, CP measurement is considered as one of the important variables in fuel research [62]. The diagrams showing the changes in CPs as a function of Crankshaft Angle (CA) resulting from the combustion of test fuels in a single-cylinder engine at a constant engine speed of 1500 rpm and different engine loads are presented in Figure 7. Start of Injection (SOI) for all fuels was determined as 337 °CA since the fuel injectors were mechanically on and off in the test setup. A sudden increase in CP was observed for all fuel samples owing to improved combustion during the uncontrolled combustion phase. After diesel fuel, HSOB has better combustion characteristics than all other fuels, and this is also reflected in CP values. Maximum CP values for D100 and B20 at full load were determined as 83.12 bar and 83.00 bar at 367 °CA, respectively. Although the fuels with the highest oxygen content are pentanol, hexanol and heptanol blends, respectively, it is thought that the maximum CPs decreased due to lower cetane numbers and heating values than B20 and D100 fuels. Furthermore, the maximum CP of B20Pe30 fuel, which had the lowest heating value despite having the highest oxygen content, with 80.57 bar, which was lower than all other fuels, supports this idea. It was determined that CP values of each fuel increased depending on the increase in the engine load (Fig. 8).

A ranking was formed as D100 > B20 > heptanol blended fuels > hexanol blended fuels > pentanol blended fuels for the maximum CP values. The same ranking is also valid for the heating value and cetane number, which are fuel characteristics that significantly affect the combustion data. The cooling effects of alcohols negatively affected the combustion characteristics. With the increase of alcohol content in the fuel blend, this effect increased further and worsened the combustion, resulting in a decrease in maximum CP. Furthermore, the maximum CP values were negatively affected since the increase in the alcohol content in the fuel blend decreased the heating values and cetane numbers of the fuels. This negative effect was also supported by the increase in the latent heat of evaporation [63].

3.2.2 Heat Release Rate

The net HRR derived using the first law of thermodynamics is a function of CP [64]. HRR is an important combustion parameter for defining combustion stages such as premixed combustion/rapid combustion/controlled combustion/post-combustion period [65]. HRR graphs showing the variation of the heat generated as a result of combustion in the cylinder with CA at full load are presented in Figure 9. The sudden burning (uncontrolled burning) phase started from °CA, which was the start of combustion, when the ignition delay period ended, and there was a rapid increase in the HRR value. Furthermore, the maximum HRR data were obtained at this stage of combustion.

The maximum HRR values obtained at different engine loads and the °CAs formed are presented in Figure 10. Maximum HRR data between 352 °CA and 359 °CA were obtained for all engine loads. Furthermore, it was seen that the maximum HRR data increased due to the increase in the amount of heat released as a result of combustion with the increase of engine load. Moreover, it was also seen that

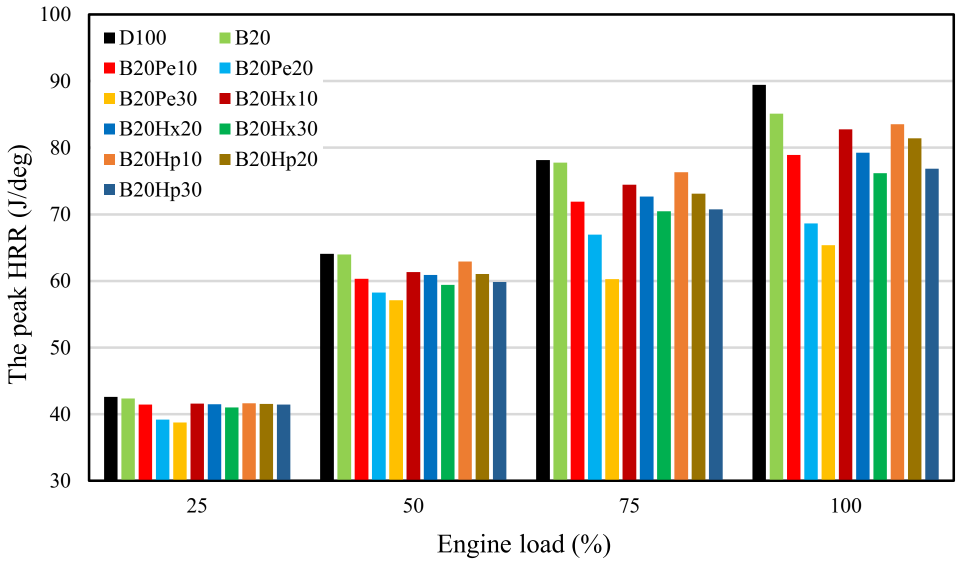

Figure 10. The peak HRR diagram of test fuels.

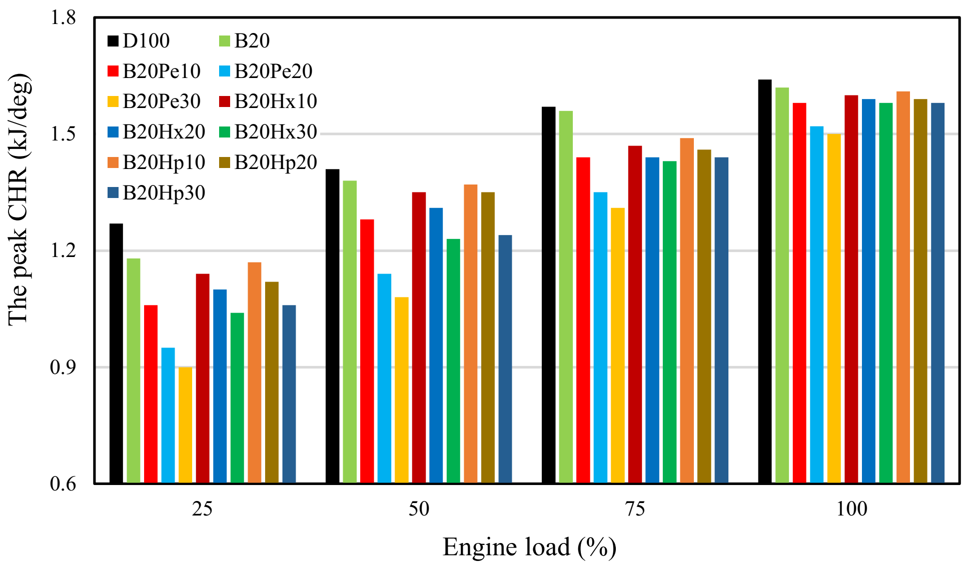

Figure 11. Diagram of the peak CHR of test fuels.

the maximum HRR values decreased as the alcohol content in the alcohol-containing fuel blends increased for all engine loads. The maximum HRR value for alcohol-containing fuels at full load was obtained at 352 °CA for B20Hp10, 355 °CA for B20Pe20 and B20Pe30, and 353 °CA for all other alcohol-containing fuels. The maximum HRR values were determined as 83,54 J/°, 82,75 J/°, 81,42 J/°, 79,24 J/°, 78,90 J/°, 76,85 J/°, 76,17 J/°, 68,62 J/°, 65,35 J/°, respectively, for B20Hp10, B20Hx10, B20Hp20, B20Hx20, B20Pe10, B20Hp30, B20Hx30, B20Pe20 and B20Pe30.

The addition of alcohol to the diesel–biodiesel fuel blend caused a decrease in the cetane number compared to both D100 and B20, which caused the ignition delay time to be longer and delayed the start of combustion. Furthermore, the decrease in the heating value of the fuels due to the increase in the alcohol content, and the increase in the cooling effect of the alcohols also had a negative impact on the maximum HRR values. When similar studies were examined, it was observed that the increase in alcohol ratios in diesel, biodiesel and alcohol ternary fuel blends decreased the cetane number and heating value of the fuels, and this caused a decrease in HRR values [27, 65].

3.2.3. Cumulative heat release

The ratio between the cumulative net heat released per cycle and the energy available in the fuel introduced into the combustion chamber indicates the efficiency of the combustion process. Combustion efficiency is an indicator of how well the thermal energy of the fuel will be transformed into heat release during the combustion process [44]. Therefore, CHR naturally increased with the increase in motor load [66]. The graph created with the maximum cumulative heat release (CHRm) values for all fuel samples tested at different engine loads is presented in Figure 11. The CHR averages of D100 and B20 fuels at all engine loads were determined as 1.47 kJ and 1.44 kJ, respectively. Among the fuels tested, D100 had the highest CHR values due to its better calorific value and effective thermal efficiency. B20 provided lower CHR values at lower crankshaft angles (except full load) compared to D100. It can be stated that the possible reasons for it were the lower calorific value of B20 compared to D100, its high viscosity and density, and the natural oxygen content in its molecular bond [67].

The alcohol blends tested presented lower CHR values compared to D100 and B20. Among alcohol blends, the highest CHR data were obtained in B20Hp10 fuel. The ranking in fuels with the same alcohol ratio was fuels containing heptanol > hexanol > pentanol. This ranking is also the same as the calorific value and cetane number and the opposite with the latent heat of vaporization. In general, as a result of the low calorific value of alcohols, the total heat released decreased, which was supported by the cooling effect of alcohols. When the CHR averages of alcohol-containing fuels at all engine loads were evaluated, the resulting ranking was B20Hp10 > B20Hx10 > B20Hp20 > B20Hx20 > B20Pe10 > B20Hp30 > B20Hx30 > B20Pe20 > B20Pe30. Considering this ranking and the maximum CHR values given in Figure 11, it can be indicated that the increase in alcohol content in the fuel blend caused a decrease in CHR values [53].

3.2.4 Ignition Delay

ID, which is one of the most important combustion parameters for diesel engines, is used to express the time between the Start Of Injection (SOI) when the fuel is sprayed from the injector towards the end of the compression period and the time until the Start Of Combustion (SOC) [65]. ID is usually associated with fuel properties such as cetane number, latent heat of vaporization and viscosity. Of these properties, the cetane number is inversely proportional to the ID period [68, 69].

The point where the curve of each fuel on the HRR diagram crossed the 0 °CA line was considered as SOC [70]. ID, SOI, SOC and End-Of-Combustion (EOC) values at different engine loads for all test fuels are presented in Table 4. The fuel SOI of the test engine was set to 337 °CA (23 °CA before TDC) as standard so that the ID time could be found. In the table, it is seen that the SOI values remained constant, while the SOC and ID values decreased depending on the increase in engine load for each fuel. This was thought to be due to the temperature of the cylinder wall and the temperature of the residual gases in the cylinder. Furthermore, one of the reasons for the decrease in ID times when the engine load is increased is the increase in the maximum Mean Gas Temperatures (MGT) [27]. The increase in engine load caused an increase in both EGT and MGTs.

It can be said that the addition of alcohol to diesel fuel and biodiesel/diesel fuel blend caused an increase in ID values. Among alcohol blended fuels, the fact that B20Hp10 gave higher ID values than B20 although it had higher heating value and cetane number than B20 fuel can be explained by the high latent heat of vaporization of B20Hp10. Furthermore, the lower ID value of B20Hp10 fuel compared to B20 can be explained by the high cooling effect of heptanol, considering the lower MGT and EGT values. ID values of D100, B20, B20Pe10, B20Pe20, B20Pe30, B20Hx10, B20Hx20, B20Hx30, B20Hp10, B20Hp20 and B20Hp30 fuels at full load were found to be 3 °CA, 4 °CA, 5 °CA, 7 °CA, 7 °CA, 5 °CA, 6 °CA, 8 °CA, 5 °CA, 6 °CA and 7 °CA, respectively. Although the heating value and cetane number of the fuels decreased due to the increase in the alcohol content in the fuel blend, the latent heat of vaporization and cooling effect increased, which resulted in the prolongation of the ID periods [65].

3.2.5. Fuel Line Pressure

Fuel Line Pressure (FLP) and the start of fuel injection are affected by the changes in fuel properties such as compressibility. SOI can also be changed with adjustments to the fuel injection pump. Fuel SOI is usually taken as the time the injector needle lifts from its seat. Since fuel injection is done with fuel pressure in mechanical fuel injection systems, FLP change will affect SOI timing and accordingly ID and SOC [71]. Since there is no needle lift sensor in the test setup used in this study, the timing at which FLP reaches the injector nozzle opening pressure (200 bar) was taken as SOI. Accordingly, the SOI used in the tests was constant at 23 °CA before TDC. FLP values for each test fuel are given in Figure 12. Since the physicochemical properties of each fuel are different and different amounts of fuel are injected, a different FLP value was found for all fuels [72]. Relatively higher FLP values were obtained by using B20 instead of D100. This was thought to be due to the higher viscosity and density values of B20 compared to D100. There were similar results for other test fuels. It can be observed that the fuel line pressure increases with the increase in engine load due to the higher amount of fuel flowing through the fuel line at higher engine loads [73].

3.2.6 Mean gas temperature

The average gas temperature is a combination of the cylinder temperature of the burned and unburned gases in the combustion chamber in the diesel cycle [74]. The maximum MGT variations at different engine loads are presented in Figure 13. For all test fuels, the maximum MGT values increased with the increase in engine load. In diesel engines, more fuel needs to be taken into the cylinder to increase the engine load. In this case, more fuel evaporates in the cylinder and there is an increase in MGT [75]. The maximum MGT values of all fuels were taken in the range of 380–384 °CA. The average of the maximum MGT values of

Table 4. Start of combustion, end of combustion and ignition delay data of test fuel.

	Engine load	D100	B20	B20Pe10	B20Pe20	B20Pe30	B20Hx10	B20Hx20	B20Hx30	B20Hp10	B20Hp20	B20Hp30
SOC (°)	25%	343	344	345	347	347	345	346	348	345	346	347
	50%	342	343	344	346	346	344	345	347	344	344	346
	75%	341	341	343	345	345	343	344	345	343	343	345
	100%	340	341	342	344	344	342	343	345	342	343	344
EOC (°)	25%	393	393	395	400	400	394	395	397	394	394	395
	50%	392	393	396	401	401	392	394	399	392	392	397
	75%	389	392	394	401	402	393	394	398	392	393	398
	100%	392	393	395	401	403	394	395	395	394	395	396
ID (°)	25%	6	7	8	10	10	8	9	11	8	9	10
	50%	5	6	7	9	9	7	8	10	7	7	9
	75%	4	4	6	8	8	6	7	8	6	6	8
	100%	3	4	5	7	7	5	6	8	5	6	7

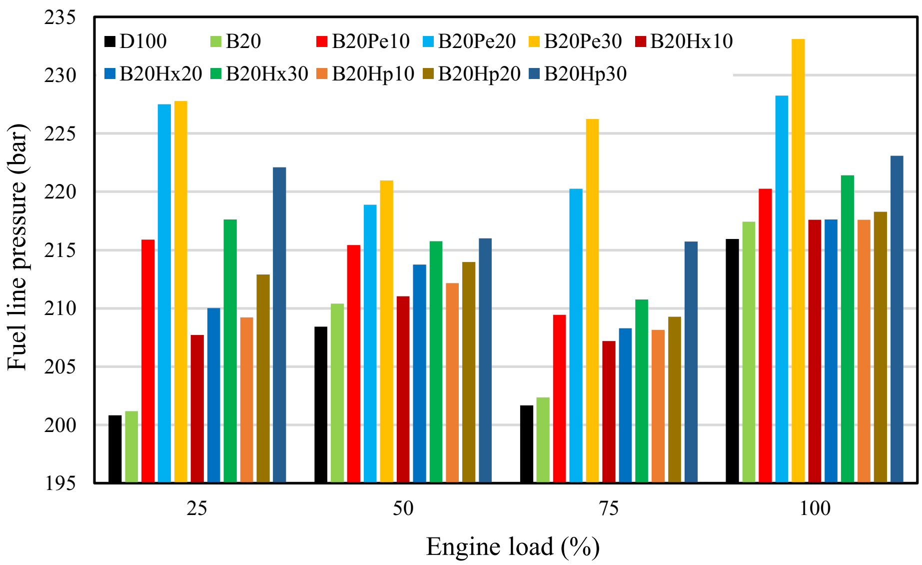

Figure 12. Fuel line pressure diagram of test fuels.

B20 fuel, which has a lower energy content than D100 fuel, was found to be 1.72% lower than D100. Among the ternary blends with pentanol, hexanol and heptanol blends, B20Pe10 fuel gave the highest maximum MGT average. Then, the highest maximum MGT averages were obtained for B20Hx10 and B20Hp fuels. When these results and the maximum MGT in Figure 13 and EGT in Figure 6 were examined, it was thought that the cooling effect of alcohols had an effect on the data. It can be concluded that the latent heat of vaporization was effective on heat production, since the latent heats of evaporation of pentanol, hexanol, and heptanol were 308.05 kJ, 486 kJ/kg, and 574.95 kJ/kg, respectively, and a similar sequence occurred in the maximum MGT values [74].

3.3 Exhaust emission results

In this section, NO_X, CO_2, CO, HC, O_2, and smoke opacity exhaust emission parameters of D100, B20, B20Pe10, B20Pe20, B20Pe30, B20Hx10, B20Hx20, B20Hx30, B20Hp10, B20Hp20 and B20Hp30 test fuels were analyzed and discussed in detail.

3.3.1 CO emission

CO emission, which is one of the most important exhaust gases in internal combustion engines, is an indicator of the insufficient combustion process in the cylinder due to insufficient amount of air in the fuel/air mixture in the cycle or insufficient time to achieve combustion reaction in the engine [76, 77]. In Figure 14 showing the CO results for all test fuels, it is seen that D100 fuel emitted more CO emissions than any other fuel. It was thought that the weak combustion characteristics caused an increase in CO emissions due to the low increase in in-cylinder temperature at low loads [78]. The decrease in CO emission values when B20 fuel was used instead of D100 can be explained by the fact that B20 fuel reduced the air-fuel ratio due to its

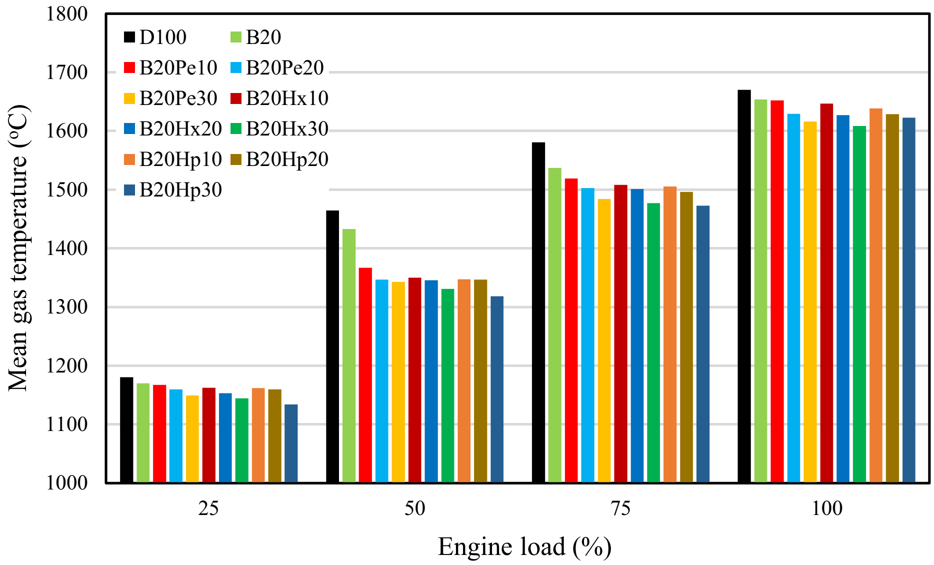

Figure 13. Mean gas temperatures of test fuels.

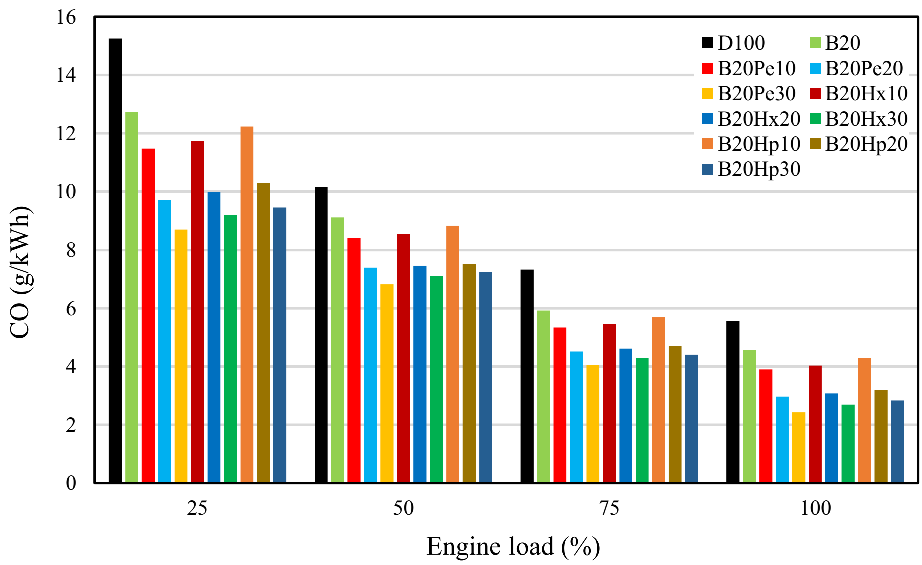

Figure 14. CO emissions from test fuels.

natural oxygen content, and consequently increased the CO_2 emissions while reducing the CO emissions [53].

CO emissions were measured at lower values in alcohol-added fuels compared to D100 and B20 fuels. The lowest CO emission values were measured as 2.429 g/kW h, 2.695 g/kW h, 2.829 g/kW h, 2.962 g/kW h, 3.071 g/kW h and 3.18 g/kW h, respectively, in B20Pe30, B20Hx30, B20Hp30, B20Pe20, B20Hx20 and B20Hp20 fuels. As can be seen, the CO emissions decreased with the increase in the amount of alcohol. Moreover, there was an order of pentanol, hexanol and heptanol from the lowest to the highest according to the amount of alcohol. This was thought to be due to the fact that pentanol, hexanol and heptanol had an oxygen content of 18.26%, 15.74% and 14.13%, respectively, reduced BTE due to the cooling effect of alcohols, and the latent heat of evaporation. Similar results have been reported by many researchers [79, 80].

3.3.2 CO_2 emission

CO_2 emission is considered as one of the undesired emissions in terms of its contribution to global warming. CO_2 is known as an important emission for internal combustion engines because it expresses the complete combustion process of the fuel, and also because it is the final combustion product of fuels containing carbon molecules in their chemical structure [81]. The variation of CO_2 emission levels depending on engine load for all fuel samples tested in this

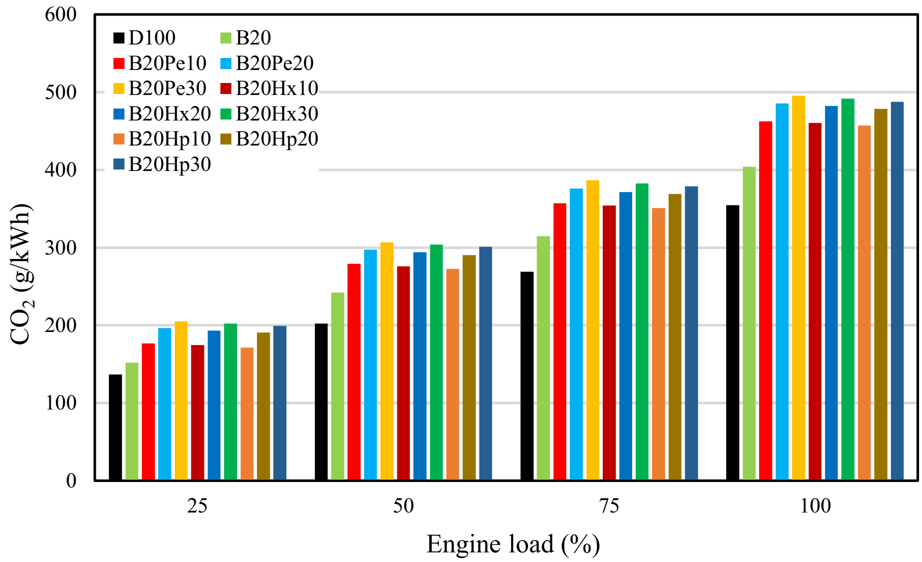

Figure 15. CO_2 emissions from test fuels.

study is presented in the graphs in Figure 15. It is seen in the graphs that CO_2 emissions increased along with the increase of engine load. The increase in BTE with engine load can be associated with this increase in CO_2 emissions [27]. In addition to the oxygen in the air taken into the cylinder at the intake time, other fuel blends except for D100 provided higher CO_2 emission values than D100 because of the oxygen content in their structures. The lowest CO_2 emission values after D100 were measured for B20 fuel. Thanks to the oxygen molecules in the chemical bonds of pentanol, hexanol and heptanol, they react with CO molecules without any problems and form CO_2 molecules. It is thought that the increase in the amount of alcohol in B20 causes an increase in the oxygen molecules, resulting in less HC and CO emissions, and has a significant impact on the increase in CO_2 emissions. Largely similar results were obtained with results reported by other researchers [82, 83].

3.3.3 HC emission

It is reported that the main causes of HC emission in diesel engines under normal operating conditions are the mixing of the fuel to be weaker than the lean mixture combustion limit during the ignition delay period, and the inability to burn some of the fuel as a result of insufficient mixing of the fuel due to the fuel injecting from the injector nozzle at low speed or at the end of the combustion process [84]. Therefore, HC emission refers to the lost chemical energy that cannot be fully converted into current work in internal combustion engines [85].

The graphs of unburned HC emissions for all fuel samples tested as a function of engine load are presented in Figure 16. The HC emission levels for the D100 occurred at the highest of all engine loads among other test fuels. This can be explained by the high BTE and the high hydrogen and carbon content due to the absence of oxygen molecules. The lower HC emission of B20 fuel than D100 can be attributed to the oxygen content of the biodiesel molecule and the lower volatility of B20 compared to D100 [84]. As the alcohol content in the ternary blends increased, HC emissions decreased further. The HC emissions of the fuels formed by the addition of pentanol to the B20 fuel were less than the fuels with the addition of hexanol and heptanol. The average HC emission values of fuels containing pentanol for each engine load were obtained as 0.059 g/kW h, 0.087 g/kW h, 0.124 g/kW h, and 0.124 g/kW h, respectively, for 25%, 50%, 75%, and 100% engine loads. Compared to fuels containing pentanol, 3.98%, 3.82%, 1.88%, and 2.16% more HC emissions were measured in fuels containing hexanol, and 6.82%, 6.87%, 4.3%, and 3.9% more HC emissions were measured in fuels containing heptanol. This can be explained by the fact that the oxygen content of pentanol was 13.8% higher than hexanol and 22.6% higher than heptanol, and the latent heat of evaporation of pentanol was 57.8% lower than hexanol and 86.6% lower than heptanol [86].

3.3.4 O_2 emission

The measurement results of O_2, which is not a harmful emission, are used to explain some parameters [82]. The transition from rich mixture to poor mixture range during combustion is analyzed by using the O_2 emission, which expresses the oxidation amount of test fuels [59]. The variation of O_2 emissions for four different engine loads of ternary blends formed by adding D100 and B20 as reference fuels and adding pentanol, hexanol and heptanol is presented in Figure 17. A decreasing trend was detected in O_2 emission due to the increase in engine load and the increase in in-cylinder temperatures. Less O_2 emissions were measured for the D100 fuel compared to all other fuels. In fact, D100 provided 4.8%, 3.2%, 7.5% and 18.6% lower O_2 emission values at 25%, 50%, 75% and 100% engine loads, respectively, than B20, that provided the closest values. This situation was thought to be caused by the oxygen molecule in the structure of all fuel concentrations

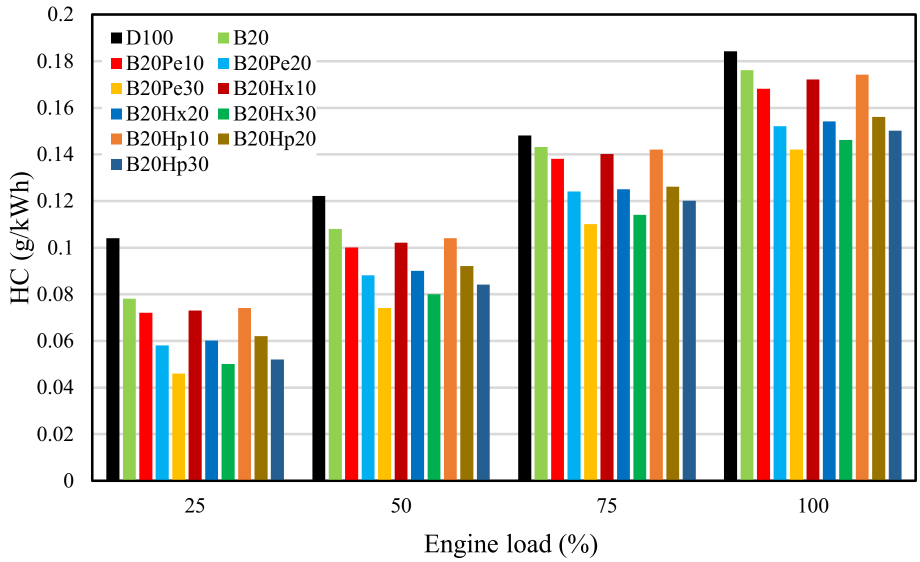

Figure 16. HC emissions from test fuels.

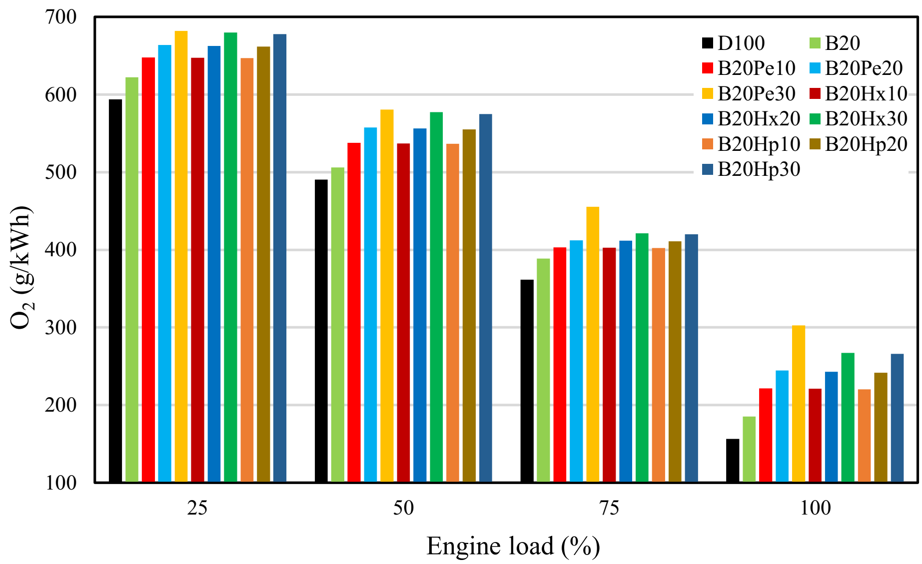

Figure 17. O_2 emissions from test fuels.

except D100. Therefore, the amount of O_2 emission also increased as the alcohol content of the blended fuels increased. The highest O_2 emission values at full load were determined as 681,819 g/kW h, 679,768 g/kW h and 677,716 g/kW h, respectively, for B20Pe30, B20Hx30 and B20Hp30 with the highest alcohol content. Largely similar results are also seen in the studies published by other researchers [78, 87].

3.3.5 NO_X emission

The nitrogen content of the air is approximately 78% and it is known that nitrogen does not react under normal conditions. However, due to high temperatures in the combustion chamber, N_2 and O_2 may react and lead to thermal (Zeldovich) nitrogen oxide (NO_X) emission, which is harmful to the environment. The NO_X values also increase when the residence time of mixtures under high temperature is prolonged [88]. Since NO_X is considered as the most harmful exhaust gas for diesel engines, it must be reduced using appropriate techniques [48].

The variation of nitrogen oxide (NO_X) emissions of test fuels at four different engine loads is presented in Figure 18. When the NO_X emission results obtained from the engine tests were evaluated, an increase in NO_X emissions was observed in all test fuels according to the engine load since the increase in the engine load caused an increase in the in-cylinder temperature. This can also be confirmed by

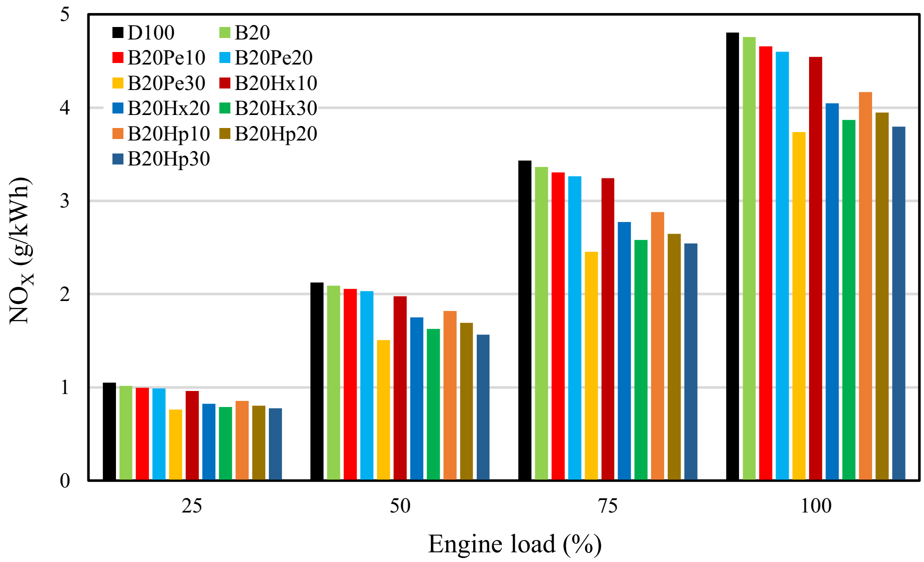

Figure 18. NO_X emissions from test fuels.

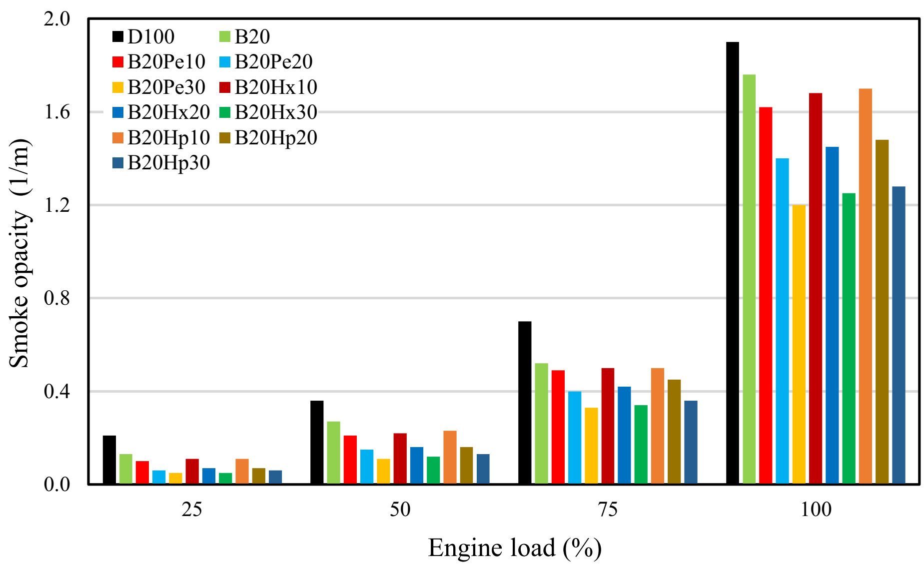

Figure 19. Smoke emissions from test fuels.

the EGT results presented in Figure 5. Among the fuel samples tested at different engine loads, the highest NO_X emission was measured for the D100 fuel. Nevertheless, due to the natural oxygen molecules in the chemical structure of B20, NO_X emission values after D100 fuel were measured at all engine loads. The addition of alcohol to B20 fuel resulted in lower NOx emissions compared to B20. This is thought to be due to the cooling effect caused by the high latent heats of vaporization of the alcoholic fuel mixtures during the combustion process [63]. When these values measured at full load for all alcohol mixtures were compared with D100, it was observed that the NO_X emissions decreased between 3.04% and 22.24%.

3.3.6 Smoke opacity

Smoke formation in diesel engines, fuel viscosity, C/H ratio, fuel injection timing, available oxygen concentration during combustion, fuel concentration at the moment of ignition and atomization quality of the fuel are the parameters affecting smoke formation [89]. The degree to which the smoke blocks light was measured as the smoke opacity value. The variation of the smoke opacity values of the fuels tested at different engine loads is presented in the graphs in Figure 19. It was observed that smoke emissions increased with the increase of engine loads due to the formation of more fuel-rich regions in the cylinder with increasing in-cylinder temperatures [90]. The highest smoke emissions

Table 5. Comparison of alcohol addition to biodiesel–diesel mixture.

Parameter	Present study	[41]	[63]	[66]	[67]	[83]	[91]	[92]	[93]	[94]	[95]
Type of test engine	1-cylinder, 4-stroke, water-cooled, naturally aspirated	1-cylinder, 4-stroke, air-cooled, naturally aspirated	1-cylinder, 4-stroke, air-cooled, naturally aspirated	1-cylinder, 4-stroke, air-cooled, naturally aspirated	1-cylinder, 4-stroke, naturally aspirated	1-cylinder, 4-stroke, water-cooled, naturally aspirated	1-cylinder, 4-stroke, water-cooled, naturally aspirated	1-cylinder, 4-stroke, air-cooled, naturally aspirated	4-cylinder, 4-stroke, water-cooled, naturally aspirated	1-cylinder, 4-stroke, air-cooled, naturally aspirated	1-cylinder, 4-stroke, water-cooled, naturally aspirated
Test conditions	– 25%, 50%, 75% and 100% engine loads –1500 rpm constant engine speed	– At constant engine speed of 3000 rpm at engine loads of 0 W, 500 W, 750 W, 1000 W and 1250 W	– 1500 rpm at constant engine speed –At 0, 10, 25, 50, 75 and 100% engine loads	– Engine loads of -2.5 Nm, 5 Nm, 7.5 Nm and 10 Nm –1500 rpm at constant engine speed	– 1500 rpm at constant engine speed –25%, 50%, 75% and 100% engine loads	– 1500 rpm at constant engine speed –At 0, 10, 25, 50, 75 and 100% engine loads	– 1500 rpm at constant engine speed –25%, 50%, 75% and 100% engine loads	– 1500 rpm constant engine speed – 0%, 25%, 50%, 75% and 100% engine loads	– 1500 rpm at constant engine speed –At 25%, 50% and 75% engine loads	– 0%, 25%, 50% and 75% engine loads –1500 rpm constant engine speed	– 0%, 25%, 50%, 75% and 100% engine loads –1500 rpm constant engine speed
Reference fuel	Diesel	Diesel	Diesel	Diesel	Diesel	Diesel	Diesel	Diesel	Diesel	Diesel	Diesel
Biodiesel feedstock	Hemp seed	Safflower seed	*Calophyllum inophyllum*	Cottonseed	Jatropha	Waste sunflower oil	Calophyllum Inophyllum	Moringa oleifera	Safflower seed	Waste cooking oil	Pongamia and mahua oil
Alcohol type	Pentanol, hexanol and heptanol	Ethanol, iso-propanol, butanol and iso-pentanol	Pentanol and octanol	Methanol, ethanol and butanol	Pentanol	Pentanol and hexanol	Hexanol and decanol	Hexanol	Propanol, pentanol, butanol and octanol	Butanol, heptanol and octanol	Ethanol and heptanol

(Continued on next page)

Table 5. (Continued)

Parameter	Present study	[41]	[63]	[66]	[67]	[83]	[91]	[92]	[93]	[94]	[95]
Fractions of alcohol (vol)	10, 20 and 30	10	10, 20, 30 and 40	10	10, 20, 30 and 40	5 and 10	30 and 40	5, 10 and 15	20	10	10 and 20
BSFC	↑	↑	↑	↑	↑	↑	↑	↑	↑	↑	↑
BSEC	↑	↑	↑	–	↑	↑	↑	↑	↑ Except 25% engine load	–	–
BMEP	↓	–	–	–	–	–	–	–	–	–	–
BTE	↓	↓	↓	↓	↓	↓	↓	↓	↑ Except 25% engine load	↓	↓
EGT	↓	↓	–	–	–	–	–	–	–	↓	↓
NO_X	↓	↓	↑	↑	↓	↓	↑	↓	↓	↓	↑
CO_2	↑	↓	–	–	–	↑	–	↑	↓	↓	↑
CO	↓	↓	↓	↓	–	↓	↓	↓	↓	↓	↓
HC	↓	↓	↓	↑	↓	↓	↓	↓	↑ Except for octanol	–	↓
O_2	↑	–		–	–	–	–	–	↑	↑	
Smoke	↓	↓	↓	↓	↓	↓	↓	↓	–	↓	↓
ID	↑	↓	↑ pentanol	↑	↓	↓	↓	↓	–	↑	↑
CP_m	↓	↓	↓	↑	↓ Except 40%	↓	↓	↓	↓	↓	↓
HRR_m	↓	↓	↓	↑	↓	↓	↓	–	↓	↑	↓
CHR_m	↓	–	–	–	–	–	↓	–	–	↓	–
FLP	↑	–	–	–	–	–	–	–	–	–	–
MGT_m	↓	–	–	–	–	–	–	–	↓	–	–

at all engine loads were measured when the engine was run on D100 fuel. Since B20 fuel, which is prepared by adding biodiesel to diesel fuel, contains O_2, smoke emissions were reduced by an average of 15.5% compared to D100 fuel.

According to the smoke emission results measured at all engine loads, as the alcohol content in the mixtures increased, the smoke emission results decreased further with the increase in the oxygen content. The smoke emissions of fuels containing pentanol were lower compared to fuels containing hexanol and heptanol. The average smoke emission values of fuels containing pentanol for each engine load were measured as 0.07 1/m, 0.157 1/m, 0.407 1/m and 1.407 1/m, respectively, for 25%, 50%, 75% and 100% engine loads. Compared to the fuels containing pentanol, the smoke emission averages of the fuels containing hexanol and heptanol were found to be 4.1% and 6.7% lower, respectively. This was thought to be due to the fact that the oxygen content of the fuels, which facilitates complete combustion, was ranked as fuels containing pentanol, hexanol and heptanol. There are many studies with similar results [19, 91].

3.3.7 Comparison of result with recent literature

The results obtained from this study were found to be similar to the studies in the literature. However, the use of higher alcohols with 5–7 carbon atoms in chemical bonds in this study distinguishes the study from others. The results obtained in this study and the research studies on ternary blends composed of diesel, biodiesel and alcohol are presented in Table 5 comparatively.

4 Conclusion

Biodiesel, which can be obtained from renewable raw materials and has environmental advantages, has become attractive for diesel engines. Furthermore, the options such as the inclusion of different alcohols in the fuel blend in various proportions can be considered as fuel substitutes in diesel engines. In this experimental study, the engine characteristics of ten dissimilar fuels consisting of diesel–HSOB (B20) and diesel–HSOB-high carbon alcohol (B20Pe10, B20Pe20, B20Pe30, B20Hx10, B20Hx20, B20Hx30, B20Hp10, B20Hp20 and B20Hp30) blends were compared with the reference diesel fuel. The test engine, which was fueled with ternary blends without any modification, ran smoothly in the tests. The main conclusions observed as a result of the experimental study are as follows:

- For all fuels, as the engine load increased, the BSFC decreased due to weak in-cylinder turbulence at low engine loads and high inertia forces in the engine's moving parts. Due to the lower calorific value and cetane number of B20 fuel, the amount of fuel consumed in order to maintain the same load condition increased and therefore the BSFC increased. Similarly, BSFC consumption was slightly increased in ternary blends. The increase in alcohol content in the fuel blend resulted in an increase in the amount of fuel consumed and a decrease in BSFC.
- The highest BTE values were obtained for D100, B20, B20Hx10 and B20Hp10 fuels at full load. Inverse values were observed between BTE and BSFC and BSEC, and directly proportional values were observed between EGT and BMEP. In general, BTE values decreased with the increase of alcohol content in fuel blends since it decreased the cetane number and calorific value.
- While CO, HC, NO_X and smoke emissions of B20 fuel were lower compared to D100, CO_2 and O_2 emissions were reflected in the measurement results with higher values. As the engine load increased, HC, CO_2, NO_X and smoke emissions increased, however, CO and O_2 emissions decreased. Among the alcohol blended fuels, the lowest smoke, CO, NO_X and HC emission values were determined in the B20Pe30 fuel. The lowest CO_2 emission values for alcohol blended fuels were found at 25% engine load in the B20Hp10 fuel. In parallel with their oxygen content, the smoke emissions of fuels containing pentanol were measured at lower values compared to fuels containing hexanol and heptanol.
- While the maximum CP values for all fuels increased in direct proportion to the engine load, the highest maximum CP values were obtained at full load and 5–7 °CA after TDC. While the highest maximum CP values were obtained as 83.12 bar and 83 bar, respectively, for D100 and B20, it was determined as 82.87 bar in the B20Hp10 fuel. The lowest maximum CP values were determined as 80.57 bar in the B20Pe30 fuel.
- As the alcohol content increased in all alcohol-containing blends, the ID times increased due to the decrease in the cetane number and calorific value, which had a negative effect on the maximum CP values.
- It was determined that the maximum FLP data changed depending on the amount of fuel, viscosity and density. PRR values changed in parallel with the engine load. The increase and decrease curves of the fuels in the graphs of the maximum MGT and EGT values are similar.
- It was observed that the maximum HRR and CHR data increased due to the increase in the amount of heat released as a result of combustion with the increase of the engine load. In general, it was determined that the cooling effect of alcohols increased in direct proportion to the increase in the alcohol content of the fuel, which negatively affected the maximum HRR and CHR results.

The results of this experimental research study reveal that pentanol, hexanol and heptanol, which act as suitable additives due to their significant benefits in emission results without pessimistic compromise in engine performance and combustion characteristics, may be a suitable oxygen-containing additive for diesel or biodiesel. This study can be extended to examine vibration and noise analysis with the same fuels or with different proportional arrangements. By conducting long-term engine tests, the effects of HSOB and higher alcohols on the mechanical parts of the engine, fuel system and lubricating oil can be examined.

Furthermore, the data from the flow/temperature of the intake air, fuel temperature, changing the injection advance and changing the injection pressure can be analyzed.

References

1 Sarıkoç S., Örs İ., Ünalan S. (2020) An experimental study on energy-exergy analysis and sustainability index in a diesel engine with direct injection diesel-biodiesel-butanol fuel blends, *Fuel* **268**.

2 BP (2019) *BP Statistical Review of World Energy*, United Kingdom, London.

3 Kalam M.A., Masjuki H.H., Jayed M.H., Liaquat A.M. (2011) Emission and performance characteristics of an indirect ignition diesel engine fuelled with waste cooking oil, *Energy* **36**, 1, 397–402.

4 Viswanathan K., Ashok B., Pugazhendhi A. (2020) Comprehensive study of engine characteristics of novel biodiesel from curry leaf (*Murraya koenigii*) oil in ceramic layered diesel engine, *Fuel* **280**, 118586.

5 Ashok B., Nanthagopal K., Chyuan O.H., Le P.T.K., Raje N., Raj A., Tamilvanan A. (2020) Multi-functional fuel additive as a combustion catalyst for diesel and biodiesel in CI engine characteristics, *Fuel* **278**, 118250.

6 Tamilvanan A., Balamurugan K., Ashok B., Selvakumar P., Dhamotharan S., Bharathiraja M., Karthickeyan V. (2021) Effect of diethyl ether and ethanol as an oxygenated additive on *Calophyllum inophyllum* biodiesel in CI engine, *Environ Sci Pollut Res* **28**, 26, 33880–33898.

7 Karthickeyan V., Ashok B., Thiyagarajan S., Nanthagopal K., Geo V.E., Dhinesh B. (2020) Comparative analysis on the influence of antioxidants role with *Pistacia khinjuk* oil biodiesel to reduce emission in diesel engine, *Heat Mass Transfer* **56**, 4, 1275–1292.

8 Papagiannakis R.G., Krishnan S.R., Rakopoulos D.C., Srinivasan K.K., Rakopoulos C.D. (2017) A combined experimental and theoretical study of diesel fuel injection timing and gaseous fuel/diesel mass ratio effects on the performance and emissions of natural gas-diesel HDDI engine operating at various loads, *Fuel* **202**, 675–687.

9 Geng L., Xiao Y., Li S., Chen H., Chen X. (2021) Effects of injection timing and rail pressure on particulate size-number distribution of a common rail DI engine fueled with Fischer-Tropsch diesel synthesized from coal, *J. Energy Inst.* **95**, 219–230.

10 Demirbas A. (2009) Progress and recent trends in biodiesel fuels, *Energy Convers. Manag.* **50**, 1, 14–34.

11 Atabani A.E., Silitonga A.S., Badruddin I.A., Mahlia T.M.I., Masjuki H., Mekhilef S. (2012) A comprehensive review on biodiesel as an alternative energy resource and its characteristics, *Renewable Sustainable Energy Rev.* **16**, 4, 2070–2093.

12 Thangaraj B., Solomon P.R. (2020) Scope of biodiesel from oils of woody plants: A review, *Clean Energy* **4**, 2, 89–106.

13 Rashid U., Ibrahim M., Yasin S., Yunus R., Taufiq-Yap Y.H., Knothe G. (2013) Biodiesel from *Citrus reticulata* (mandarin orange) seed oil, a potential non-food feedstock, *Industrial Crops Products* **45**, 355–359.

14 Carolan M.S. (2009) Environmental review: the cost and benefits of biofuels: A review of recent peer-reviewed research and a sociological look ahead, *Environmental Practice* **11**, 1, 17–24.

15 Gui M.M., Lee K.T., Bhatia S. (2008) Feasibility of edible oil *vs.* non-edible oil *vs.* waste edible oil as biodiesel feedstock, *Energy* **33**, 11, 1646–1653.

16 Leizer C., Ribnicky D., Poulev A., Dushenkov S., Raskin I. (2000) The composition of hemp seed oil and its potential as an important source of nutrition, *J. Nutraceuticals funct. Med. Foods* **2**, 4, 35–53.

17 Wei M., Li S., Liu J., Guo G., Sun Z., Xiao H. (2017) Effects of injection timing on combustion and emissions in a diesel engine fueled with 2, 5-dimethylfuran-diesel blends, *Fuel* **192**, 208–217.

18 Khalife E., Tabatabaei M., Demirbas A., Aghbashlo M. (2017) Impacts of additives on performance and emission characteristics of diesel engines during steady state operation, *Prog. Energy Combust. Sci.* **59**, 32–78.

19 Kumar B.R., Saravanan S. (2016) Use of higher alcohol biofuels in diesel engines: a review, *Renewable Sustainable Energy Rev.* **60**, 84–115.

20 Togbe C., Dagaut P., Mzé-Ahmed A., Diévart P., Halter F., Foucher F. (2010) Experimental and detailed kinetic modeling study of 1-hexanol oxidation in a pressurized jet-stirred reactor and a combustion bomb, *Energy Fuels* **24**, 11, 5859–5875.

21 De Poures M.V., Sathiyagnanam A.P., Rana D., Kumar B.R., Saravanan S. (2017) 1-hexanol as a sustainable biofuel in DI diesel engines and its effect on combustion and emissions under the influence of injection timing and Exhaust Gas Recirculation (EGR), *Appl. Therm. Eng.* **113**, 1505–1513.

22 Nour M., Sun Z., El-Seesy A.I., Li X. (2021) Experimental evaluation of the performance and emissions of a direct-injection compression-ignition engine fueled with N-hexanol–diesel blends, *Fuel* **302**, 121144.

23 Sathiyagnanam A.P., Saravanan C.G., Gopalakrishnan M. (2010) Hexanol-ethanol diesel blends on DI-diesel engine to study the combustion and emission, *Proceedings of the World Congress on Engineering*, **2**, 1–5

24 Raju V.D., Kumar K.K., Kishore P.S. (2016) Engine performance and emission characteristics of a direct injection diesel engine fuelled with 1-hexanol as a fuel additive in Mahua seed oil biodiesel blends, *Int. J. Thermal Environ. Eng.* **13**, 2, 121–127.

25 Karlapudi S., Gardas R.L., Sivakumar K. (2013) FT-IR Studies on Excess Thermodynamic Properties of Binary Liquid Mixtures O-Chlorotoluene with 1-Propanol, 1-Butanol, 1-Pentanol, 1-Hexanol and 1-Heptanol At Different Temperatures, *the Journal of Chemical Thermodynamics* **67**, 203–209.

26 Devarajan Y., Munuswamy D.B., Radhakrishnan S., Mahalingam A., Nagappan B. (2019) Experimental testing and evaluation of neat biodiesel and heptanol blends in diesel engine, *J. Test. Eval.* **47**, 2, 987–997.

27 Yesilyurt M.K. (2020) A detailed investigation on the performance, combustion, and exhaust emission characteristics of a diesel engine running on the blend of diesel fuel, biodiesel and 1-heptanol (C7 alcohol) as a next-generation higher alcohol, *Fuel* **275**, 117893.

28 Marcheschi R.J., Li H., Zhang K., Noey E.L., Kim S., Chaubey A., Houk K.N., Liao J.C. (2012) A synthetic recursive "+1" pathway for carbon chain elongation, *ACS Chem. Biol.* **7**, 4, 689–697.

29 Immethun C.M., Henson W.R., Wang X., Nielsen D.R., Moon T.S. (2016) Engineering central metabolism for production of higher alcohol-based biofuels, in: *Biotechnology for Biofuel Production and Optimization*, Elsevier, pp. 1–34.

30 Sarathy S.M., Oßwald P., Hansen N., Kohse-Höinghaus K. (2014) Alcohol combustion chemistry, *Prog. Energy Combust. Sci.* **44**, 40–102.

31 Dogan B., Cakmak A., Yesilyurt M.K., Erol D. (2020) Investigation on 1-heptanol as an oxygenated additive with diesel fuel for compression-ignition engine applications: an approach in terms of energy, exergy, exergoeconomic, enviroeconomic, and sustainability analyses, *Fuel* **275**, 117973.

32 Nour M., Nada S., Li X. (2022) Experimental study on the combustion performance of a stationary CIDI engine fueled with 1-heptanol-diesel mixtures, *Fuel* **312**, 122902.

33 El-Seesy A.I., He Z., Kosaka H. (2021) Combustion and emission characteristics of a common rail diesel engine run with n-heptanol-methyl oleate mixtures, *Energy* **214**, 118972.

34 Pandian A.K., Munuswamy D.B., Radhakrishanan S., Devarajan Y., Ramakrishnan R.B.B., Nagappan B. (2018) Emission and performance analysis of a diesel engine burning cashew nut shell oil bio diesel mixed with hexanol, *Pet. Sci.* **15**, 1, 176–184.

35 John C.B., Raja S.A. (2020) Analysis of combustion, emission and performance attributes of hemp biodiesel on a compression ignition engine, *World Rev. Sci. Technol. Sustain. Develop.* **16**, 2, 169–183.

36 Sridhar R., Jeevahan J., Chandrasekaran M. (2020) Effect of the addition of 1-pentanol on engine performance and emission characteristics of diesel and biodiesel fuelled single cylinder diesel engine, *Int. J. Ambient Energy* **41**, 1, 58–63.

37 Pardo C., Pabon J., Fonseca Vigoya M. (2021) Analysis of the characteristics of combustion, emissions, and energy efficiency of blends of heptanol with pure diesel fuel in compression ignition engine, *Int. J. Energy Convers. (IRECON)* **9**, 5, 221–229.

38 Yesilyurt M.K., Cesur C. (2020) Biodiesel synthesis from *Styrax officinalis* L. seed oil as a novel and potential non-edible feedstock: A parametric optimization study through the Taguchi technique, *Fuel* **265**, 117025.

39 Priyadarshi D., Paul K.K. (2019) Optimisation of biodiesel production using Taguchi model, *Waste Biomass Valorization* **10**, 6, 1547–1559.

40 Yilbaşi Z., Yesilyurt M.K., Arslan M. (2021) The production of methyl ester from industrial grade hemp (*Cannabis Sativa* L.) seed oil: A perspective of turkey – the optimization study using the Taguchi method, *Biomass Convers. Biorefinery* 1–21.

41 Yesilyurt M.K., Aydin M., Yilbasi Z., Arslan M. (2020) Investigation on the structural effects of the addition of alcohols having various chain lengths into the vegetable oil-biodiesel-diesel fuel blends: an attempt for improving the performance, combustion, and exhaust emission characteristics of a compression ignition engine, *Fuel* **269**, 117455.

42 Dhawane S.H., Kumar T., Halder G. (2016) Biodiesel Synthesis from *Hevea brasiliensis* oil employing carbon supported heterogeneous catalyst: Optimization by Taguchi method, *Renewable Energy* **89**, 506–514.

43 Campos-Fernandez J., Arnal J.M., Gomez J., Lacalle N., Dorado M.P. (2013) Performance tests of a diesel engine fueled with pentanol/diesel fuel blends, *Fuel* **107**, 866–872.

44 Nour M., Attia A.M., Nada S.A. (2019) Combustion, performance and emission analysis of diesel engine fuelled by higher alcohols (butanol, octanol and heptanol)/diesel blends, *Energy Convers. Manage.* **185**, 313–329.

45 Çakmak A., Yeşilyurt M.K., Erol D., Doğan B. (2022) The experimental investigation on the impact of N-octanol in the compression-ignition engine operating with biodiesel/diesel fuel blends: Exergy, exergoeconomic, environmental analyses, *J. Therm. Anal. Calorim.* **147**, 20, 11231–11259.

46 Van Gerpen J.H., Peterson C.L., Goering C.E. (2007) *Biodiesel: An alternative fuel for compression ignition engines*, American Society of Agricultural and Biological Engineers, Kentucky, USA, pp. 1–22.

47 Yeşilyurt M., Arslan M., Eryılmaz T. (2018) Biyodizel-Dizel Yakıt Karışımlarına Etanol Katılmasının Performans, Yanma ve Emisyon Karakteristiklerine Etkilerinin Deneysel İncelenmesi, *Isı Bilimi ve Tekniği Dergisi* **38**, 2, 129–150.

48 Yesilyurt M.K., Cakmak A. (2021) An Extensive Investigation of Utilization of a C8 type long-chain alcohol as a sustainable next-generation biofuel and diesel fuel blends in a CI Engine – the effects of alcohol infusion ratio on the performance, exhaust emissions, and combustion characteristics, *Fuel* **305**, 121453.

49 Santhosh K., Kumar G.N., Sanjay P.V. (2020) Experimental analysis of performance and emission characteristics of CRDI diesel engine fueled with 1-pentanol/diesel blends with EGR technique, *Fuel* **267**, 121453.

50 Lamani V.T., Yadav A.K., Gottekere K.N. (2017) Performance, emission, and combustion characteristics of twin-cylinder common rail diesel engine fuelled with butanol-diesel blends, *Environ. Sci. Pollut. Res.* **24**, 29, 23351–23362.

51 Verma P., Dwivedi G., Behura A.K., Patel D.K., Verma T. N., Pugazhendhi A. (2020) Experimental investigation of diesel engine fuelled with different alkyl esters of Karanja Oil, *Fuel* **275**, 117920.

52 Holman J.P. (2012) *Experimental methods for engineers.*

53 Ramesh A., Ashok B., Nanthagopal K., Pathy M.R., Tambare A., Mali P., Phuke P., Patil S., Subbarao R. (2019) Influence of hexanol as additive with *Calophyllum inophyllum* biodiesel for CI engine applications, *Fuel* **249**, 472–485.

54 Fattah I.R., Kalam M.A., Masjuki H.H., Wakil M.A. (2014) Biodiesel production, characterization, engine performance, and emission characteristics of Malaysian Alexandrian Laurel Oil, *RSC Adv.* **4**, 34, 17787–17796.

55 Paul A., Bose P.K., Panua R., Debroy D. (2015) Study of performance and emission characteristics of a single cylinder CI engine using diethyl ether and ethanol blends, *J. Energy Inst.* **88**, 1, 1–10.

56 Yesilyurt M.K., Aydin M. (2020) Experimental investigation on the performance, combustion and exhaust emission characteristics of a compression-ignition engine fueled with cottonseed oil biodiesel/diethyl ether/diesel fuel blends, *Energy Conver. Manage.* **205**, 112355.

57 Rajendran R., Gomez J.P.U., Javed M.M., Subbiah G. (2020,) Reduction of NOx emissions with low viscous biofuel using exhaust gas recirculation technique, *AIP Conf. Proc.*, Vol. **2311**, December, AIP Publishing LLC., p. 020026.

58 Sundar R.C., Saravanan G. (2011) Influence of hexanol-diesel blends on constant speed diesel engine, *Thermal Sci.* **15**, 4, 1215–1222.

59 Suhaimi H., Adam A., Mrwan A.G., Abdullah Z., Othman M.F., Kamaruzzaman M.K., Hagos F.Y. (2018) Analysis of combustion characteristics, engine performances and emissions of long-chain alcohol-diesel fuel blends, *Fuel* **220**, 682–691.

60 Shrivastava P., Verma T.N., Pugazhendhi A. (2019) An experimental evaluation of engine performance and emission characteristics of CI engine operated with Roselle and Karanja biodiesel, *Fuel* **254**, 115652.

61 Atmanli A. (2016) Comparative analyses of diesel-waste oil biodiesel and propanol, N-Butanol Or 1-pentanol blends in a diesel engine, *Fuel* **176**, 209–215.

62 Kumar A.N., Ashok B., Nanthagopal K., Ong H.C., Geca M.J., Victor J., Vignesh R., Jeevanantham A.K., Kannan P.S., Kishore P.S. (2020) Experimental analysis of higher alcohol-based ternary biodiesel blends in CI engine parameters through multivariate and desirability approaches, *Biomass Convers. Biorefinery* **12**, 1525–1540.

63 Nanthagopal K., Ashok B., Saravanan B., Patel D., Sudarshan B., Ramasamy R.A. (2018) An assessment on the effects of 1-pentanol and 1-butanol as additives with *Calophyllum inophyllum* biodiesel, *Energy Convers. Manage.* **158**, 70–80.

64 Ashok B., Nanthagopal K., Anand V., Aravind K.M., Jeevanantham A.K., Balusamy S. (2019) Effects of n-octanol as a fuel blend with biodiesel on diesel engine characteristics, *Fuel* **235**, 363–373.

65 Ashok B., Nanthagopal K., Saravanan B., Azad K., Patel D., Sudarshan B., Ramasamy R.A. (2019) Study on isobutanol and *Calophyllum inophyllum* biodiesel as a partial replacement in CI engine applications, *Fuel* **235**, 984–994.

66 Emiroğlu A.O., Şen M. (2018) Combustion, performance and exhaust emission characterizations of a diesel engine operating with a ternary blend (alcohol-biodiesel-diesel fuel), *Appl. Thermal Eng.* **133**, 371–380.

67 Appavu P., Venu H. (2019) Quaternary blends of diesel/biodiesel/vegetable oil/pentanol as a potential alternative feedstock for existing unmodified diesel engine: Performance, combustion and emission characteristics, *Energy* **186**, 115856.

68 Saravanan S., Nagarajan G., Rao G.L.N., Sampath S. (2010) Combustion characteristics of a stationary diesel engine fuelled with a blend of crude rice bran oil methyl ester and diesel, *Energy* **35**, 1, 94–100.

69 Murugapoopathi S., Vasudevan D. (2019) Performance, combustion and emission characteristics on VCR multi-fuel engine running on methyl esters of rubber seed oil, *J. Therm. Anal. Calorim.* **138**, 2, 1329–1343.

70 Alagumalai A. (2015) Combustion characteristics of lemongrass (*Cymbopogon flexuosus*) oil in a partial premixed charge compression ignition engine, *Alex. Eng. J.* **54**, 3, 405–413.

71 Sanli H., Canakci M., Alptekin E., Turkcan A., Ozsezen A.N. (2015) Effects of waste frying oil based methyl and ethyl ester biodiesel fuels on the performance, combustion and emission characteristics of a DI diesel engine, *Fuel* **159**, 179–187.

72 Canakci M. (2007) Combustion characteristics of a turbocharged DI compression ignition engine fueled with petroleum diesel fuels and biodiesel, *Bioresour. Technol.* **98**, 6, 1167–1175.

73 Dhar A., Agarwal A.K. (2014) Performance, emissions and combustion characteristics of Karanja biodiesel in a transportation engine, *Fuel* **119**, 70–80.

74 Santhosh K., Kumar G.N. (2020) Impact of 1-Hexanol/diesel blends on combustion, performance and emission characteristics of CRDI CI mini truck engine under the influence of EGR, *Energy Convers. Manage.* **217**, 113003.

75 Santhosh K., Kumar G.N. (2021) Effect of injection time on combustion, performance and emission characteristics of direct injection CI engine fuelled with equi-volume of 1-hexanol/diesel blends, *Energy* **214**, 118984.

76 Atmanlı A., Ileri E., Yüksel B. (2014) Experimental investigation of engine performance and exhaust emissions of a diesel engine fueled with diesel–N-butanol–vegetable oil blends, *Energy Convers. Manage.* **81**, 312–321.

77 Yilmaz N., Atmanli A., Vigil F.M. (2018) Quaternary blends of diesel, biodiesel, higher alcohols and vegetable oil in a compression ignition engine, *Fuel* **212**, 462–469.

78 Yilmaz N., Morton B. (2011) Comparative characteristics of compression ignited engines operating on biodiesel produced from waste vegetable oil, *Biomass Bioenergy* **35**, 5, 2194–2199.

79 Sharon H., Ram P.J.S., Fernando K.J., Murali S., Muthusamy R. (2013) Fueling a stationary direct injection diesel engine with diesel-used palm oil-butanol blends – an experimental study, *Energy Convers. Manage.* **73**, 95–105.

80 Li L., Wang J., Wang Z., Xiao J. (2015) Combustion and emission characteristics of diesel engine fueled with diesel/biodiesel/pentanol fuel blends, *Fuel* **156**, 211–218.

81 Imdadul H.K., Masjuki H.H., Kalam M.A., Zulkifli N.W.M., Alabdulkarem A., Rashed M.M., Teoh Y.H., How H.G. (2016) Higher alcohol–biodiesel–diesel blends: An approach for improving the performance, emission, and combustion of a light-duty diesel engine, *Energy Convers. Manage.* **111**, 174–185.

82 Pullen J., Saeed K. (2014) Factors affecting biodiesel engine performance and exhaust emissions–Part II: Experimental study, *Energy* **72**, 17–34.

83 Babu D., Anand R. (2017) Effect of biodiesel-diesel-N-pentanol and biodiesel-diesel-N-hexanol blends on diesel engine emission and combustion characteristics, *Energy* **133**, 761–776.

84 Fattah I.R., Masjuki H.H., Liaquat A.M., Ramli R., Kalam M.A., Riazuddin V.N. (2013) Impact of various biodiesel fuels obtained from edible and non-edible oils on engine exhaust gas and noise emissions, *Renewable Sustainable Energy Rev.* **18**, 552–567.

85 Pulkrabek W.W. (2004) İçten Yanmalı Motorlar Mühendislik Temelleri (1. Baskı), in: Yaşar H., Büyükkaya E., Soyhan H.S., Taymaz İ., *Engineering Fundamentals of the Internal Combustion Engine*, İzmir Güven Bookstore, İzmir, pp. 299–307.

86 Wei L., Cheung C.S., Huang Z. (2014) Effect of N-pentanol addition on the combustion, performance and emission characteristics of a direct-injection diesel engine, *Energy* **70**, 172–180.

87 Emaish H., Abualnaja K.M., Kandil E.E., Abdelsalam N.R. (2021) Evaluation of the performance and gas emissions of a tractor diesel engine using blended fuel diesel and biodiesel to determine the best loading stages, *Sci. Rep.* **11**, 1, 1–12.

88 Anderson A., Devarajan Y., Nagappan B. (2018) Effect of injection parameters on the reduction of NOx emission in neat bio-diesel fuelled diesel engine, *Energy Sources A: Recovery Util. Environ. Eff.* **40**, 2, 186–192.

89 Mohammadi P., Nikbakht A.M., Tabatabaei M., Farhadi K., Mohebbi A. (2012) Experimental investigation of performance and emission characteristics of DI diesel engine fueled with polymer waste dissolved in biodiesel-blended diesel fuel, *Energy* **46**, 1, 596–605.

90 Venu H., Madhavan V. (2017) Influence of Diethyl Ether (DEE) addition in Ethanol-Biodiesel-Diesel (EBD) and Methanol-Biodiesel-Diesel (MBD) blends in a diesel engine, *Fuel* **189**, 377–390.

91 Ashok B., Nanthagopal K., Darla S., Chyuan O.H., Ramesh A., Jacob A., Sahil G., Thiyagarajan S., Geo V.E. (2019) Comparative assessment of hexanol and decanol as oxygenated additives with *Calophyllum inophyllum* biodiesel, *Energy* **173**, 494–510.

92 Ramalingam S., Mahalakshmi N.V. (2020) Influence of *Moringa oleifera* biodiesel–diesel–hexanol and biodiesel–diesel–ethanol blends on compression ignition engine performance. Combustion and Emission Characteristics, *RSC Adv.* **10**, 8, 4274–4285.

93 Işık M.Z. (2021) Comparative experimental investigation on the effects of heavy alcohols-safflower biodiesel blends on combustion, performance and emissions in a power generator diesel engine, *Appl. Thermal Eng.* **184**, 116142.

94 Nour M., Elseesy A.I., Attia A., Li X., Nada S. (2021) Adding N-butanol, N-heptanol, and N-octanol to improve vaporization, combustion, and emission characteristics of diesel/used frying oil biodiesel blends in DICI engine, *Environ. Prog. Sustain. Energy* **40**, 3, E13549.

95 Swarna S., Swamy M.T., Divakara T.R., Krishnamurthy K.N., Shashidhar S. (2022) Experimental assessment of ternary fuel blends of diesel, hybrid biodiesel and alcohol in naturally aspirated CI engine, *Int. J. Environ. Sci. Technol.* **19**, 9, 8523–8554.